DESIGN AND EVALUATION OF MEASUREMENT INSTRUMENTATION USED FOR HIGH ENERGY TIBIA IMPACTS ON FRESH POST-MORTEM HUMAN SUBJECTS

A Thesis

Presented in Partial Fulfillment of the Requirements for

The Degree of Bachelors in Science with Distinction in the Undergraduate School

of The Ohio State University

By,

Matt Kremer

****

The Ohio State University

2009

Honors Examination Committee:

Dr. John Bolte, IV, Advisor

Dr. Yann Guezennec

Approved by

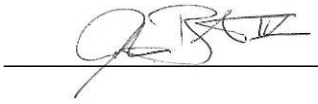

Advisor

Department of Mechanical Engineering

ABSTRACT

Injury to the medial collateral ligament (MCL) and anterior cruciate ligament (ACL) are common when knees are subjected to loading from the lateral direction. These types of injuries occur often in sports and are also common in vehicle-pedestrian collisions. Previously, the Injury Biomechanics Research Laboratory (IBRL) at The Ohio State University has developed instrumentation for anterior tibia impacts, which included instrumentation to measure the posterior cruciate ligament (PCL) stretch.

The objective of this research was to take knowledge gleamed from the frontal testing to develop an instrumentation technique for lateral impact testing of the knee, focusing on MCL and ACL stretch and injury. The goal of this study was to develop and verify instrumentation that can be used in future studies on ligament tears and avulsions on post-mortem human subjects (PMHS). This research also looked to accurately measure the angle between the tibia and the femur during impact and identify the time of injury for both ligament and bone failures. Instrumentation techniques using micro-differential variable reluctance transducers (Micro-DVRTs) were used to measure stretch in the ligaments due to the confined space within the knee joint. Accelerometers, angular rate sensors, high-speed cameras, and load cells were used to determine the angle of the femur with respect to the tibia and to measure force of impact. The initial trials included 4 PMHS denuded legs being laterally rotated by gravity until the thigh impacted a load plate causing loading across the knee. During the tests, all mounted instrumentation on the leg remained fixed and recorded the motion of the leg and the stretch of the ligaments.

From these initial tests, suturing the DVRT barbs to the ACL provided repeatable ACL displacement measurements. When the MCL is well defined, suturing the DVRT barbs to the MCL also provided repeatable MCL displacement measurements. With both MCL and ACL DVRT signals, the time of injury can be determined accurately. It was also determined that angular velocity may be a predictor of ligament injury that could be used in future work if more trials are performed and found to support this hypothesis.

Dedicated to my parents who are always there to support and encourage me.

ACKNOWLEDGEMENTS

First and I would like to thank my advisor Dr. John H. Bolte, IV, who has been extremely helpful and patient throughout this whole process. Without Dr. Bolte I would have never been introduced to the exciting field of injury biomechanics. Dr. Bolte was always willing to meet with me to discuss any questions I had about my research or classes. Dr. Bolte always went above and beyond his role as an honors advisor, by being my mentor and friend.

Next I would like to thank Rod Herriot. From the beginning Rod was extremely helpful and supportive. Rod's expertise was very helpful when it came to designing and building the testing rig needed for my research. I also want to thank Rod for all of his hard work and long hours during test days. I have learned a great deal from Rod. He has been there throughout this process and has provided me with creative solutions to the problems I encountered. I would also like to thank Ann Mallory for helping guide my research by providing her knowledge of prior pedestrian work and for her support on test days.

Next I would also like to thank Yun-Seok Kang for taking the time to teach me about matrix transformations and also for allowing me to adapt his MATLAB code for this project. Yun also took the time to teach me DIAdem while helping me with the data analysis of the project.

Finally, I would like to thank Amanda Agnew, Kyle Icke, Hannah Gustafson, Brian Suntay, Austin Meek, Matt Long, Michael Keller, Jason Miller, and Anthony Vergis for their assistance on test day. Without everyone's help test days would have been a lot longer and much more hectic than they already are.

TABLE OF CONTENTS

Abstract……...……..……..II

Dedication……..III

Acknowledgements…….IV

List of Tables…….VII

List of Figures …….……VIII

Chapters:

1. Introduction……...……..1

2. Anatomy……...……3

2.1. Bones of the Leg…….…….3

2.2. Muscles surrounding the knee……...……..……..5

2.3 Tendons of the knee…….…….…….…7

3. Previous Research…….…….……..9

4. Objective…….…….……..11

5. Methods…….…….…12

5.1. Introduction to methods……...…….……..12

5.2. 0901PED Specific Methods.…….……..18

5.3. 0902PED Specific Methods.…….…….…19

5.4. 0903PED Specific Methods……...……..21

5.5. Data Processing……...……...……..21

6. Results……...…….24

6.1. 0901PED Results……..……..24

6.2. 0902PED Results……..……..…….…...30

6.3. 0903PED Results……..……..…….....40

7. Discussion…….…….46

8. Conclusion…….48

References…….……...……..49

Appendix…….……...……51

A. Pre-Test Data Protocol……..…….……51

B. Pre-Test/Autopsy Examination Sheet……..……..…….54

C. Sample Test Checklist……..…….……..…….……..59

D. Sample Decontamination Checklist.……...…...…….65

E. Sample Instrumentation Configuration...……...……...……..67

F. Sample FARO Arm Checklist…….……..…….…….68

G. MATLAB Code……...…….…….…….……72

LIST OF TABLES

Table 1: Measured Variables and Test Devices 15

Table 2: 0901PED Test Matrix 19

Table 3: 0902PED Test Matrix 20

Table 4: 0903PED Test Matrix 21

Table 5: CFC to Low-Pass Butterworth Filter 22

Table 6: 0901PED Subject Information 24

Table 7: 0901PED Ligament Information 25

Table 8: 0901PED Initial Test Results 25

Table 9: 0902PED Subject Information 30

Table 10: Comparison of Subject's MCLs 31

Table 11: 0902PED Ligament Information 31

Table 12: 0902PED Initial Test Results 32

Table 13: 0903PED Subject Information 40

Table 14: 0903PED Ligament Information 41

Table 16: Summary of Injury Results 45

LIST OF FIGURES

Figure 1: Bones of the Leg (from: www.encarta.msn.com) 3

Figure 2: Articulating Structures of the knee [11] 4

Figure 3: Four Muscles of the Quadriceps Femoris Muscle [11] 5

Figure 4: Location of the Three Hamstring Muscles [11] 6

Figure 5: Major Ligaments of the Knee [11] 7

Figure 6: Height Definition 13

Figure 7: SAE J211 Coordinate System [11] 14

Figure 8: Figure of Setup with Instrumentation 15

Figure 9: Micro-DVRT 16

Figure 10: Micro-DVRT inserted and sutured in MCL 16

Figure 11: Micro-DVRT inserted and sutured in ACL 16

Figure 12: Femur Accelerometer and Angular Rate Sensor Block 17

Figure 13: Tibia Accelerometer Mount Attached with Gorilla Glue 17

Figure 14: Tibia Accelerometer and Angular Rate Sensor Block 17

Figure 15: Shoe with 5 lb Weight Attached to Bottom of Foot 19

Figure 16: Leg with 2.5 lb Ankle Weight Attached 20

Figure 17: FARO Locations on Accelerometer Blocks 22

Figure 18: Accelerometer Block Point Digitization 23

Figure 19: 0901PED ACL Stretch 27

Figure 20: 0901PED MCL Stretch 28

Figure 21: 0901PED Angular Rotation of Tibia 29

Figure 22: 0901PED ACL and MCL Stretch with Resultant Angular Velocity 30

Figure 23: 0902PEDR ACL Stretch 33
Figure 24: 0902PEDR MCL Stretch..... 34
Figure 25: 0902PEDR Angular Rotation of Tibia 35
Figure 26: 0902PEDR ACL and MCL Stretch with Resultant Angular Velocity..... 36
Figure 27: 0902PEDL ACL Stretch..... 37
Figure 28: 0902PEDR MCL Stretch..... 38
Figure 29: 0902PEDL Angular Rotation of Tibia 39
Figure 30: 0902PEDL ACL and MCL Stretch with Resultant Angular Velocity 40
Figure 31: 0903PED ACL Stretch 42
Figure 32: 0903PED MCL Stretch 43
Figure 33: 0903PED Angular Rotation of Tibia..... 44
Figure 34: ACL Stretch seen on Injury Trials 45

CHAPTER 1

INTRODUCTION

Accidents involving pedestrians are very common and often lead to injury to the lower extremities. Traffic accidents worldwide injure more than 430,000 pedestrians each year [12]. In United States alone, on average 78,000 pedestrians are involved in non-fatal pedestrian-vehicle collisions each year [7]. In a large portion of these collisions knee ligament injuries are sustained [2]. In published pedestrian-vehicle collision literature there is much emphasis on the effect that bumper height has on the type of injury to the lower extremities. However this literature focuses on injuries to the long bones of the lower extremities and not on the ligaments in the knee [4,5]. This lack of injury data points to a need to evaluate the effect of bumper height on the ACL/MCL ligaments in the knee.

By 2015, the European Union will demand that all automakers' products make collisions with pedestrians survivable when contacted at 40km/h. With the push from legislature, automakers are beginning to design softer car fronts that require testing to verify that the vehicles are pedestrian friendly [13]. In order to enforce these laws, accurate test devices are needed to aid the automakers with this transition. Legform impactors are commonly used as predictors for lower extremity injury during pedestrian-vehicle impacts. These impactors can be used and implemented as a legislative instrument for current and future legislations on pedestrian protection. Currently, these legform impactors use injury criterion from loading conditions not entirely representative of pedestrian impacts [15]. This fact points to a need to have instrumentation that can allow for the development of injury criterion for loading more similar to pedestrian-vehicle collisions on full body post-mortem human subjects (PMHS).

Knee injuries are also among the most economically costly sports injuries and are the leading cause of high school sports-related surgeries. Knee injuries accounted for nearly 45 percent of all sports-related surgeries. These injuries can require extensive and expensive post-surgery rehabilitation and can increase risk for early onset osteoarthritis [9].

Developing instrumentation for lateral impacts that measure ACL and MCL response on PMHS could help with research on lower limb impacts seen during pedestrian-vehicle collisions and also with the study of knee injuries to athletes documented in today's sporting world.

CHAPTER 2

ANATOMY

Section 2.1: Bones of the Leg

The femur as shown in Figure 1 is the only bone of the thigh. The femur is the longest and heaviest bone in the human body. The head of the femur articulates in a circular depression of the pelvis known as the acetabulum. The shaft of the femur has a slight curve to allow the knee joint to be in line with the body's center of gravity. The distal end of the knee joint is characterized by two rounded structures known as the medial and lateral condyles as shown in Figure 2. These femoral condyles are the articulating surfaces of the femur in the knee joint.

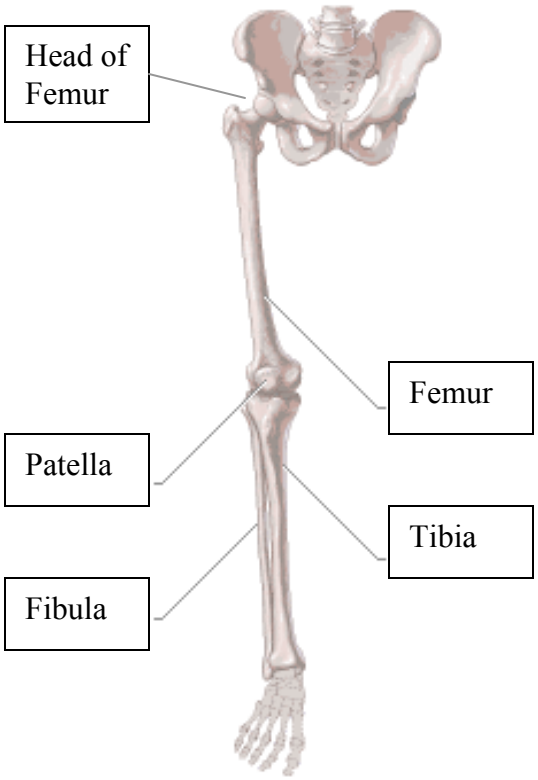

Figure 1: Bones of the Leg (from: www.encarta.msn.com)

The patella commonly known as the kneecap is located on the anterior surface of the knee joint as shown in Figure 1. The patella serves to protect the knee joint and increase the leverage of the quadriceps femoris muscle as it extends the leg at the knee.

The tibia is the main weight bearing bone of the lower leg. The proximal end (head) of the tibia is characterized by two slightly concave surfaces known as the medial and lateral condyles as shown in Figure 2. These tibial condyles are the articulating surfaces of the tibia in the knee. The proximal end of the tibia is often referred to as the tibia plateau. The tibia tuberosity is located on the anterior part of the tibia, just below the plateau, and is the attachment site of the patellar tendon.

The fibula is a long slender bone that runs parallel to the tibia as shown in Figure 1. The fibula is more important for muscle attachment than for weight bearing support.

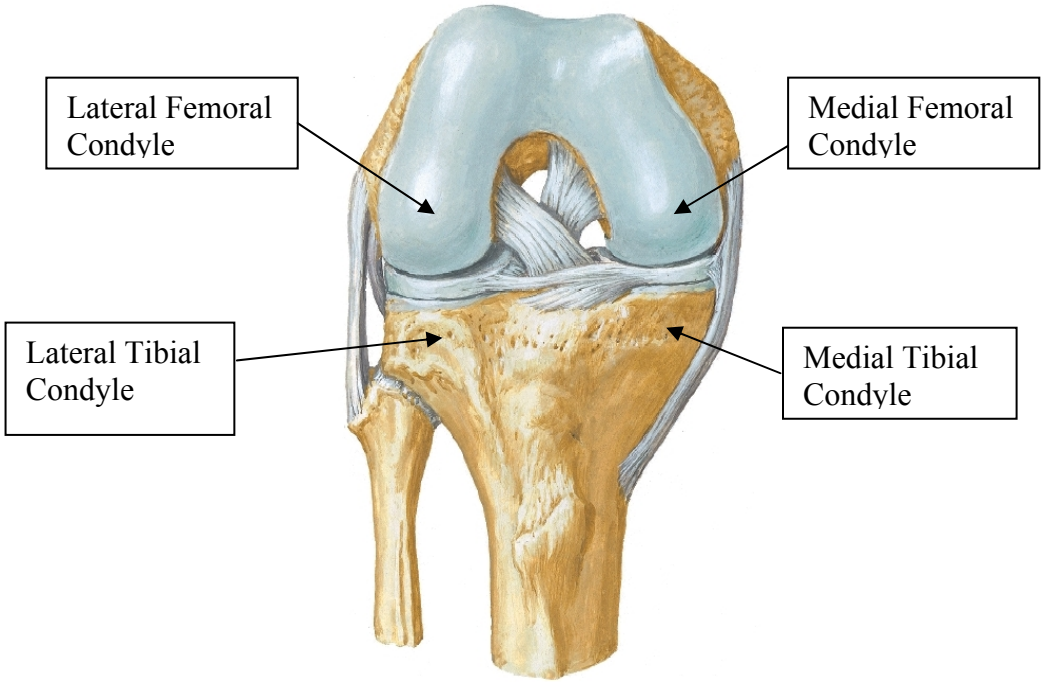

Figure 2: Articulating Structures of the knee [11]

Section 2.2 Muscles Controlling the Knee

The muscle group responsible for extending the leg at the knee is known as quadriceps femoris. Quadriceps femoris is made up of four muscles; rectus femoris, vastus lateralis, vastus medialis and vastus intermedius. All four muscles are powerful extensors of the knee joint. Rectus femoris is the most superficial of the four muscles and occupies the middle of the thigh. It attaches to the ilium (uppermost bone of the pelvis) which also makes it a flexor of the hip. Vastus lateralis is positioned laterally on the leg. Vastus medialis occupies the medial position along the thigh. Vastus intermedius lie deep to the rectus femoris. The four muscles of quadriceps femoris are shown in Figure 3.

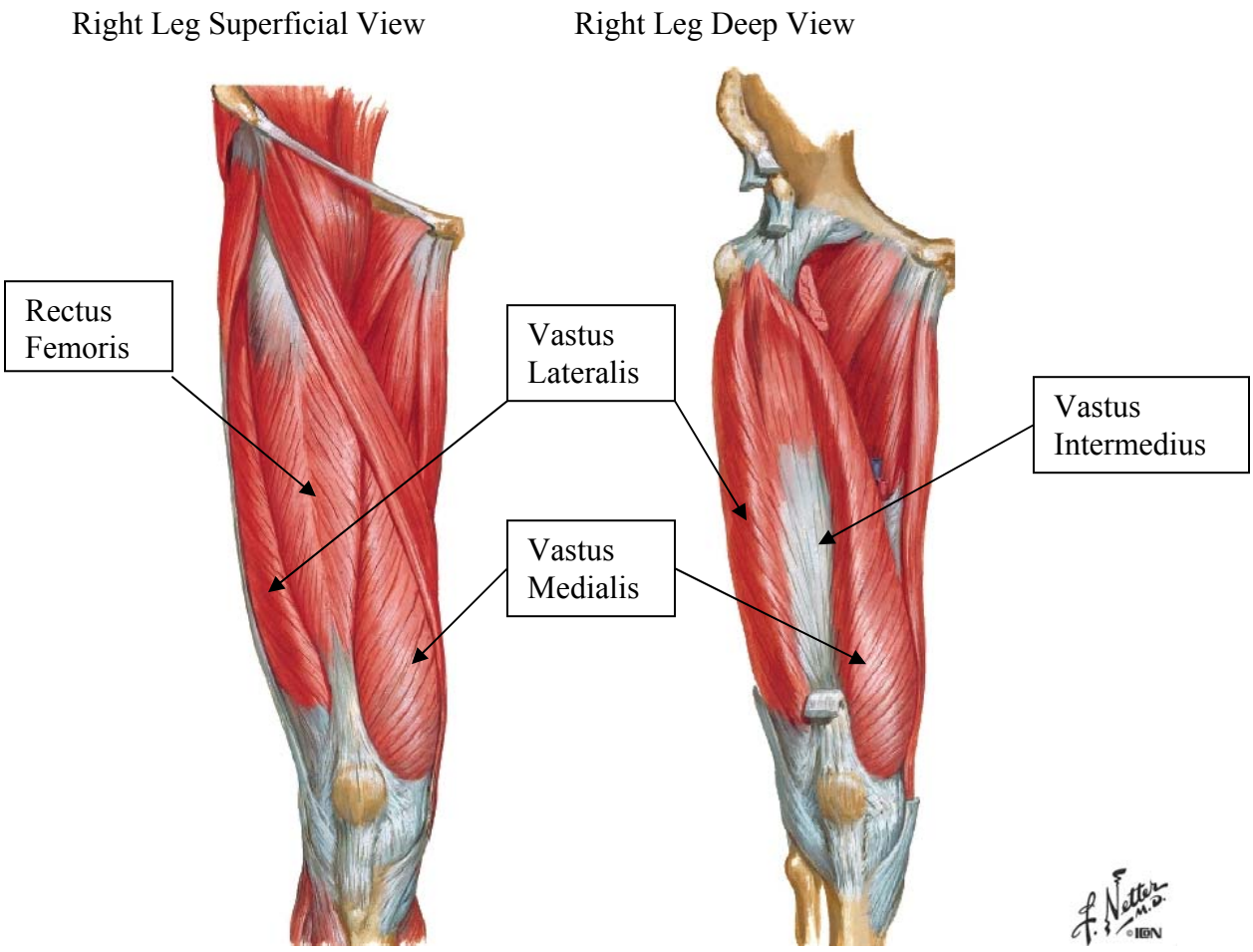

Figure 3: Four Muscles of the Quadriceps Femoris Muscle [11]

There are three muscles that are responsible for flexing the leg at the knee and extending the hip. These muscles are commonly known as the hamstring, and are located on the posterior of the thigh. Biceps femoris is located on the lateral portion of the thigh. The biceps femoris has both a short and long head. The long head of the biceps femoris originates at the ischial tuberosity (lateral boundary of the pelvic outlet) and inserts at the medial surface of the tibia. The short head of the biceps femoris originates at the linea aspera (near the head of the femur) and inserts at the lateral side of the head of the fibia sharing a common tend with the long head of the biceps femoris. Because of its location of origin the short head of the biceps femoris is not involved in hip extension. Semitendinosus is located on the posterior medial portion of the thigh and originates at the ischial tuberosity and inserts at the medial tibial condyle. Semimembranosus is located deep to semitendinosus and originates at the ischial tuberosity and inserts at the lateral side of the head of the fibula. The locations of the three hamstring muscles are shown in Figure 4.

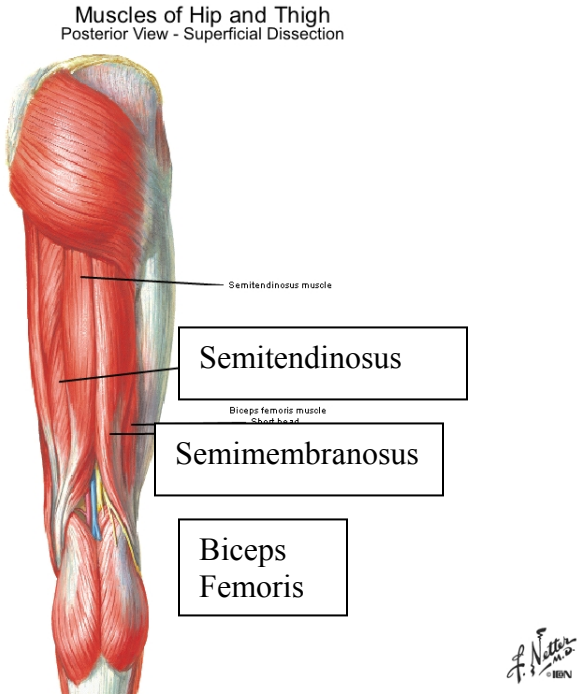

Figure 4: Location of the Three Hamstring Muscles [11]

Section 2.3 Major Tendons and Ligaments of the knee

The ligament that connects the patella to the tibial tuberosity is known as the patellar ligament. The ligaments that are responsible for stability in the anterior/posterior direction are known as the posterior cruciate ligament (PCL) and the anterior cruciate ligament (ACL). The PCL lies deep within the knee joint and runs from the anterior femur to the posterior tibia. The ACL, which lies anterior to the PCL, runs from the posterior femur to the anterior tibia. The locations of the ACL and PCL are shown in Figure 5.

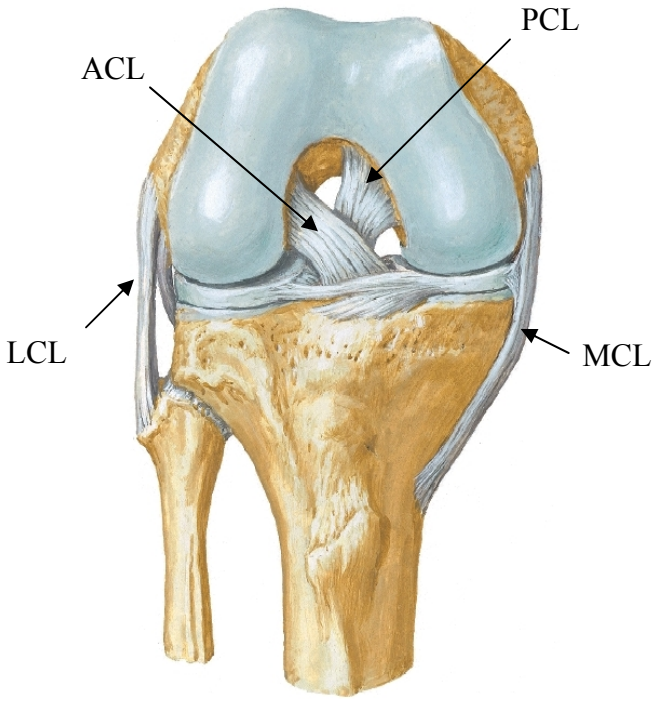

Figure 5: Major Ligaments of the Knee [11]

Ligaments only provide resistance when placed in tension. The PCL provides resistance to posterior tibia displacement relative to the femur. The ACL provides resistance to anterior tibia displacement relative to the femur. The ACL is also essential in protecting the knee from twisting, primarily inwards rotation of the tibia which is often caused by lateral impacts to the knee.

The ligaments that are responsible for the medial/lateral stability of the knee are known as the lateral collateral ligament (LCL) and the medial collateral ligament (MCL). The LCL is located on the lateral portion of the knee, connecting the femur to the fibula. The MCL is located on the medial portion of the knee, connecting the femur to the tibia. The locations of the LCL and MCL are shown in Figure 5 [10].

CHAPTER 3

PREVIOUS RESEARCH

There is a need to develop a precise measurement system that can be used to measure the strain of ligaments in humans to better understand injury and function of the knee ligaments. There have been studies that have tested the four knee ligaments at loading rates that represent typical pedestrian-vehicle collisions. These tests were used to compare actual ligament response to theoretical response [2]. However, these tests were performed on ligaments separated from the knee and not performed as impact tests on actual post-mortem human subjects (PMHS).

In published pedestrian-vehicle collision literature there is much emphasis on the effect that bumper height has on the type of injury to the lower extremities. However this literature focuses on injuries to the long bones of the lower extremities and not on the ligaments in the knee [4,5]. The main injury experience by pedestrians at an impact velocity between 20-30km/hr is to the knee ligament. At speeds closer to 40km/hr the most common injury is a fracture to the leg [3].

The Ohio State University Injury Biomechanics Research Laboratory has previously conducted high-energy anterior tibia impacts on fresh PMHS. The main focus of these studies looked at injuries to the PCL due to frontal crashes were the dashboard loads the leg. The similarity of this proposed study to the anterior PCL study leads us to hypothesize that much of the test instrumentation used previously may be used to analyze the MCL and ACL. Instrumentation such as differential variable reluctance transducers (DVRT) have been developed to measure strain in ligaments [1]. In these previous tests, due to the confined space within the knee joint, a Micro-Differential Variable Reluctance Transducer [Micro-DVRT,

MicroStrain Inc., Burlington, VT] was chosen to measure ligament displacement based on its small size and previous use in ligament displacement studies [6].

Kajzer et al conducted ten experiments on ten different PMHS's (9 male, 1 female) to study the effects that bending and shearing loading had on the knee. Kajzer et al separately ran both pure lateral shearing and pure valgus bending tests at the knee joint to create various types of injuries documented in pedestrian-automobile accidents. However these tests did not have instrumentation located on the ligaments to measure their response [8].

Because both valgus bending and shear of the knee have been identified as the primary mechanisms of injuries applicable to lateral loading seen in pedestrian-vehicle collisions, Bose et al expanded on previous work by Kajzer et al and subjected the knee to the combined effects of bending and shear loading. However, knee specimens that only included the soft tissue and surrounding flesh around the joint were tested in both 4-point and 3-point bending tests. In this study the leg was also constrained, restricting twisting of the knee [14].

Legform impactors are commonly used as predictors for lower extremity injury during pedestrian-vehicle impacts. These impactors can be used and implemented as a legislative instrument for current and future legislations on pedestrian protection. Currently, these legform impactors use injury criterion from Kajzer et al [15]. There may be a need to have instrumentation that can allow for injury criterion to be developed for combined loading on full body PMHS.

.

CHAPTER 4

OBJECTIVE

Because the knee has visco-elastic properties, the criterion for current knee injury needs to be verified by dynamic impacts using a "real world" test setup. Based on previous tibia impact tests, there is a need to evaluate the current measurement instrumentation used in measuring medial collateral ligament (MCL) and anterior cruciate ligament (ACL) stretch. The measurement instrumentation needs to allow for accurate measurements during lateral impacts to the tibia of the PMHS, without affecting the biomechanical response of the subject. Previously, The Ohio State University Injury Biomechanics Research Laboratory (IBRL) has developed instrumentation for high-energy anterior tibia impacts, including instrumentation to measure the posterior cruciate ligament (PCL) stretch in such impacts. The objective of this research is to take knowledge gleamed from the frontal testing to develop an instrumentation technique for lateral impact testing of the knee, focusing on MCL and ACL stretch. The formal objective of this research is to develop a measurement instrumentation technique that will complete the following tasks:

- Accurately measure tibial angular rotation relative to the femur
- Accurately measure both ACL and MCL stretch
- Identify the time of injury for both ligament and bone failures

CHAPTER 5

METHODS

Section 5.1 Introduction to Methods

Since September 2008, four denuded legs from a total of three PMHS have been dynamically tested at The Ohio State University Injury Biomechanics Research Laboratory. The testing was completed to verify hypothesized instrumentation techniques while also gaining insight to the biomechanical response and properties of the lower extremities when loaded laterally. Before accepting each PMHS Bone Mineral Density (BMD) testing was performed to ensure that all test subjects did not suffer from osteoporosis, and the subject's blood was tested for HIV/AIDS, Hepatitis B and Hepatitis C. No subjects with pre-existing knee injuries or surgeries were accepted for this study. Appendix A contains an example Pre-Test Protocol sheet which includes all relevant subject information. Appendix B contains an example Pre-Test and Autopsy (Post Test) Examination Sheet which ensured that inspection to each leg was performed to confirm that no prior injury to the knee had occurred to the subject. It also allowed for a detailed report of injury at autopsy for each subject. To ensure that the tests were conducted in a repeatable and efficient manor a test procedure checklist was created and can be found in Appendix C.

A standard nomenclature for the test subjects has been developed to aid in the recognition of impacts and subjects. The nomenclature used follows: ####PED##X##, where the first two numbers are the last two numbers of the year in which the test was completed. The next two numbers represent the i^{th} subject tested that year. The letters PED stand for project name which in this instance stood for pedestrian testing. The next two numbers stand for the height at which the leg was released from in inches. Tibial center of mass was estimated to

be twenty-one inches from the rotation pin and was used as reference point to measure drop height. The change in height (Δh) of this point from its free hanging position was defined as the drop height and is shown in Figure 6. The next letter denotes which leg (right or left) was used in the trial. Finally, the last two numbers represent the impact number for that leg. Due to limitations of the impact rig design, the maximum height that the leg could be released from was nineteen inches. On two out of three subjects, injury did not occur at this maximum height so trials in which weight was added to the foot of the subject were needed. For these trials an additional letter was added in the nomenclature: ####PED19WX## with the W indicating that a predetermined amount of weight was added to the foot and documented on the test matrix sheet. As an example, a test named 0901PED14R07 means that the test was conducted in 2009, the subject was the first in this project (PED), was released from a height of fourteen inches, and was the seventh impact on the right leg.

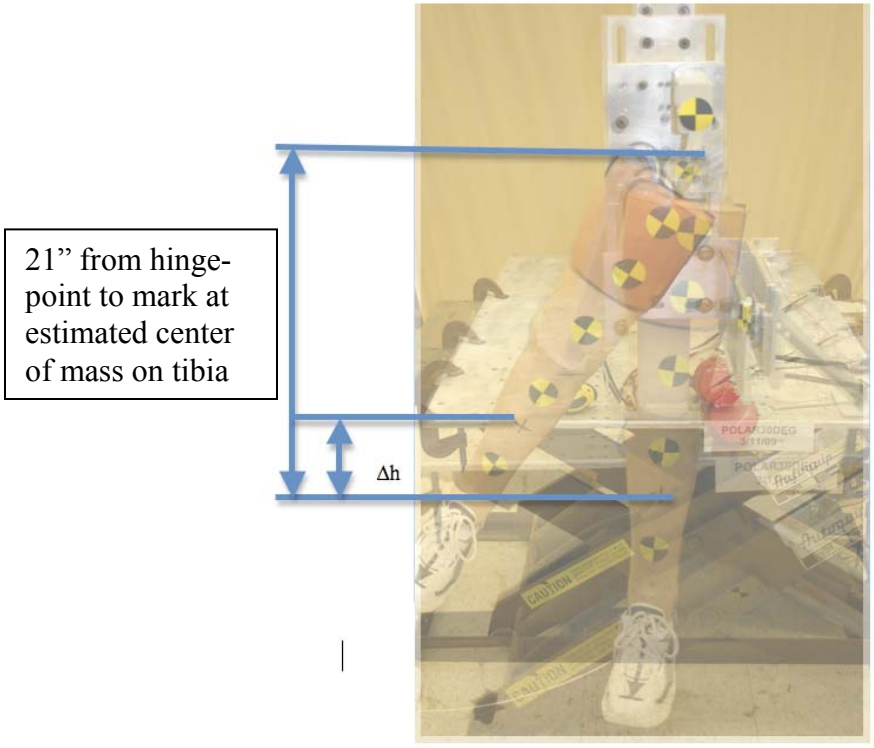

Figure 6: Height Definition

The coordinate system used in all tests is defined in the SAE J211 [10] and is the coordinate system used in crash Anthropomorphic Test Devices (ATDs). Each section of the subject has its own coordinate system that can translate or rotate with the section to which the coordinate system is designed. It is particularly important to understand this coordinate system because the orientation of the coordinate system for the femur is different depending on whether or not the leg is in the flexed position or un-flexed position. The difference in orientation is shown in Figure 7. For this research the un-flex coordinate system was used.

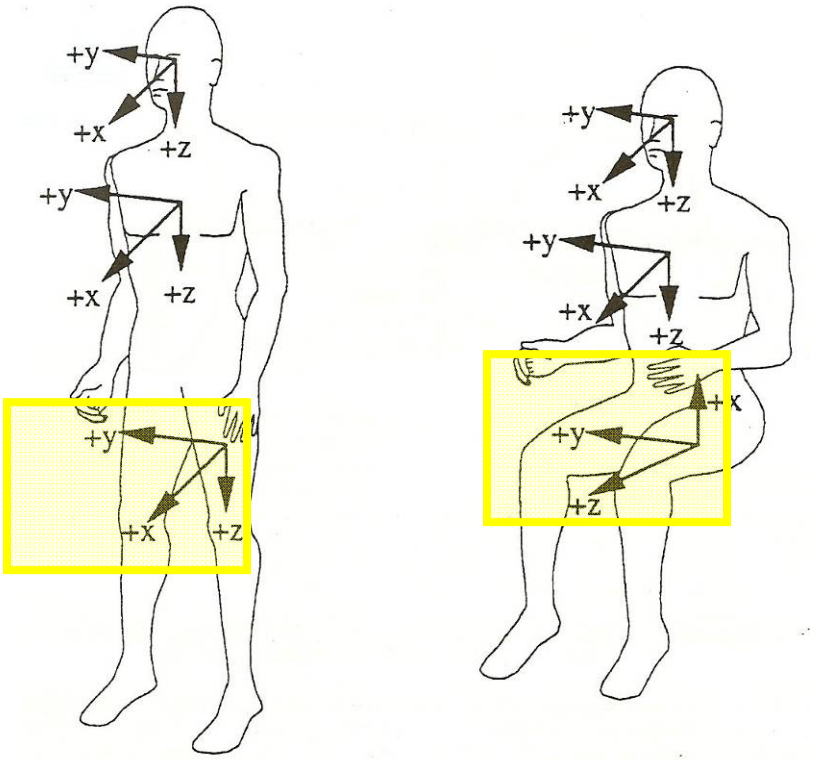

Figure 7: SAE J211 Coordinate System [11]

Each limb was raised to a predetermined height and allowed to free swing about a pivot point (similar to a pendulum) and impact a plate situated so that the impact with the leg would occur to the entire thigh and bend the leg about the lateral femoral condyle. The measured variables and the instrumentation are listed in

Table 1 and photographs of the set-up can be seen in Figure 8. The objective of this test was to determine the time of injury within the knee due to impact loading, and at that time determine the angle between femur and tibia and MCL and ACL stretch.

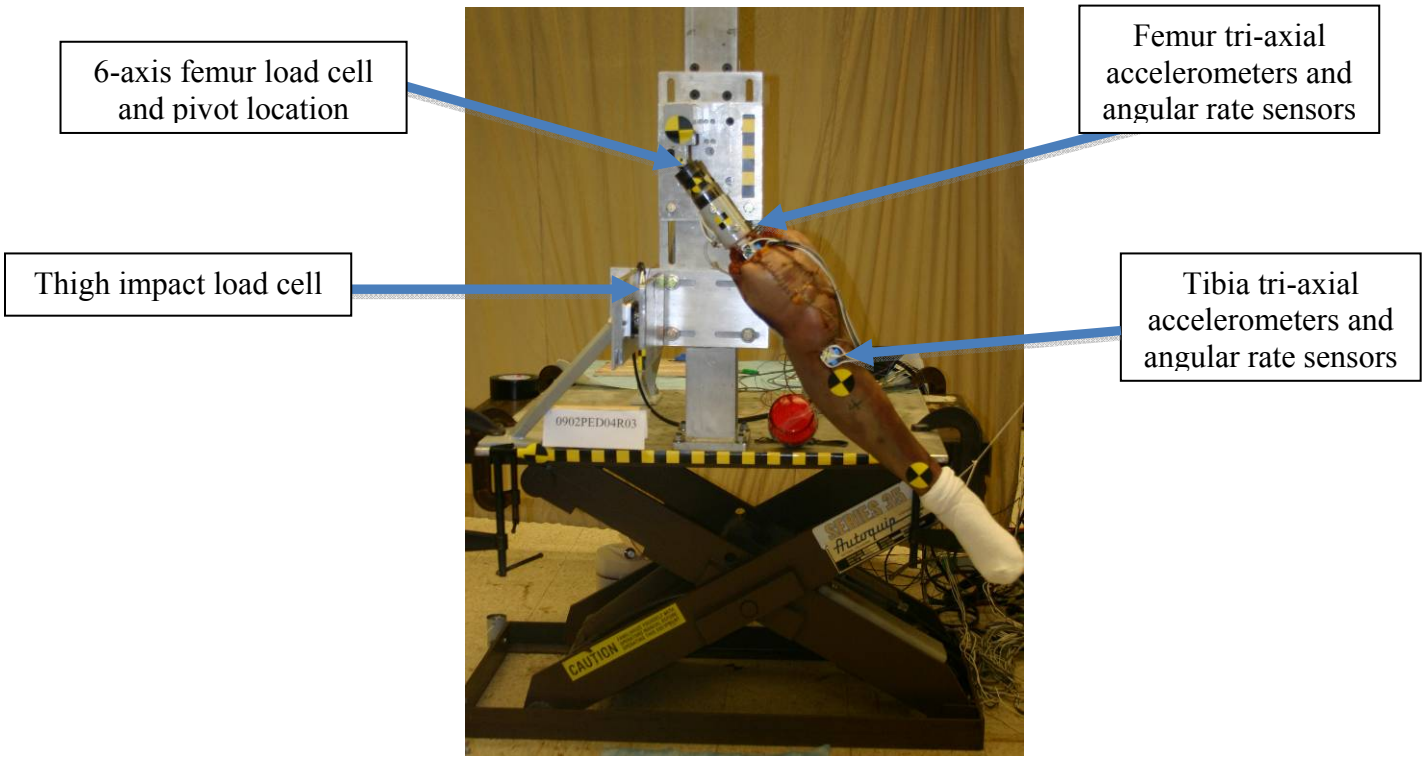

Figure 8: Figure of Setup with Instrumentation

Table 1: Measured Variables and Test Devices

Measured Value	Device
Relative Angle Between Tibia and Femur	High Speed Video Footage
Tibial Motion/Rotation	Accelerometers and Angular Rate Sensors
Femur Motion/Rotation	Accelerometers and Angular Rate Sensors
Femur Force	Six Axis Load Cell
Force at Impact Location	Six Axis Load Cell
MCL Stretch	Micro-DVRT
ACL Stretch	Micro-DVRT

Two micro-differential variable reluctance transducers (DVRT) [DEMOD-DVRT, MicroStrain Inc., Burlington, VT] were used to record displacement of both the MCL and ACL. They were attached by barbs that inserted in the fibers of the ligaments and were then sutured in place to ensure that the barbs would not be pulled out during testing. A DVRT is shown in Figure 9 and the implanted DVRTs are shown in Figure 10 and Figure 11.

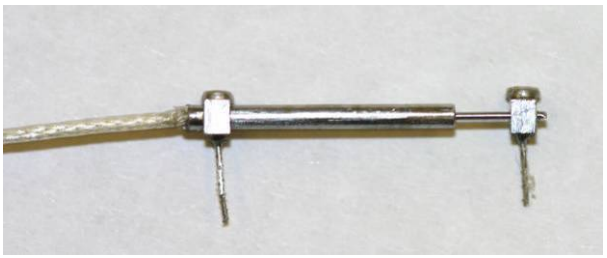

Figure 9: Micro-DVRT

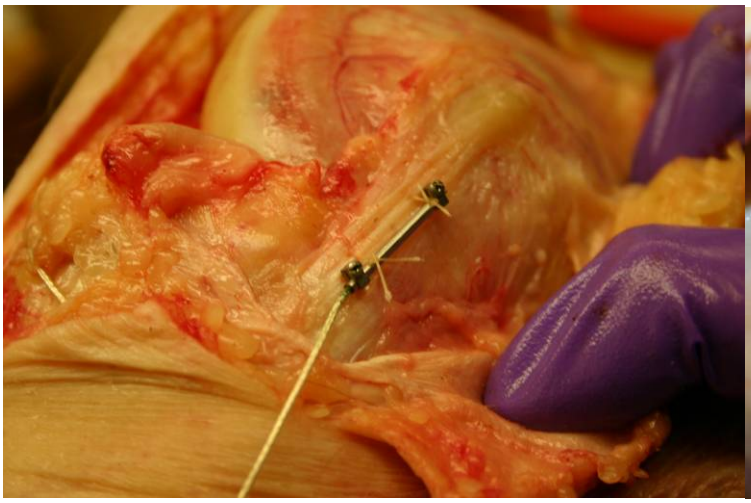

Figure 10: Micro-DVRT inserted and sutured in MCL

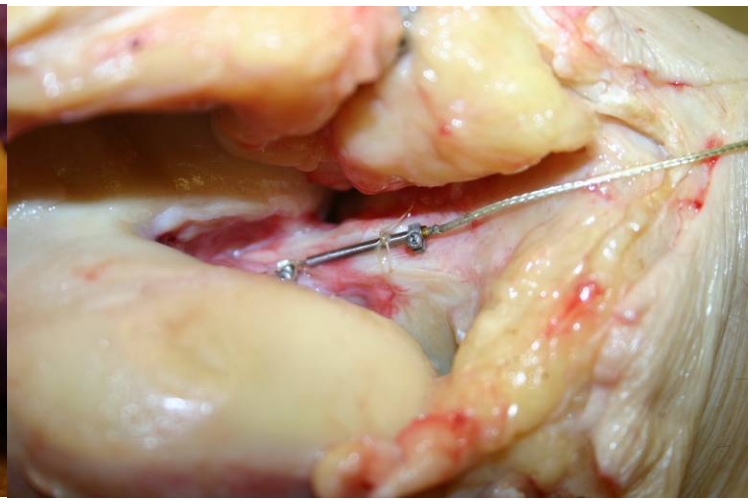

Figure 11: Micro-DVRT inserted and sutured in ACL

The legs of each PMHS were removed approximately leaving approximately eleven inches of femur attached to the knee. The femurs were then securely potted using Bondo Ultimate Filler™ [Bondo Corporation, Atlanta, GA] to the test platform, shown in Figure 12. A six-axis load cell (Model #2667 RA Denton Inc., Rochester, MI) was located inline with the femur to measure the forces and moments acting on the femur. Another six-axis load cell (Model #2944 RA Denton, Inc., Rochester, MI) was located behind the impactor plate to

measure the forces and moments acting at the impact location. Each leg was also instrumented with a 3aω motion blocks that measure acceleration and angular velocity about three axes. These blocks enabled tracking of both the motion of the femur and tibia with respect to time. In order to transform the accelerometer data into the proper coordinate system at each height, the positions of these blocks were digitized using the FARO arm (FARO Technologies, Lake Mary, FL). This will be explained further in Section 5.5 Data Processing. The block on the femur was attached to a mount held on by wire ties wrapped around the femur. The block on the tibia was attached to a mount that was glued on with Gorilla Glue to a location on the tibial tuberosity, which was flattened using a Dremel. These 3aω motion blocks and their mounts can be seen in Figure 12, Figure 13, and Figure 14.

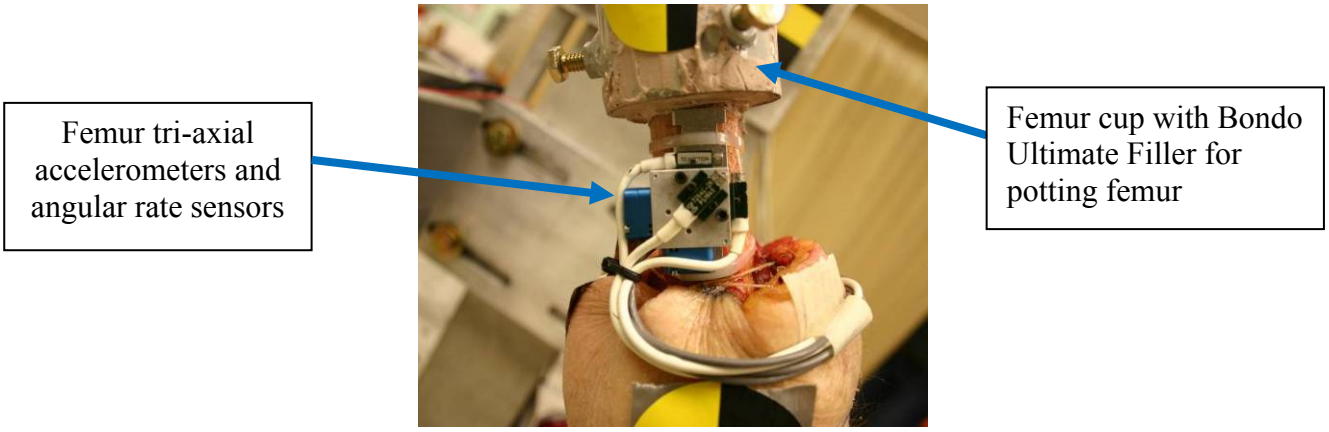

Figure 12: Femur Accelerometer and Angular Rate Sensor Block

Figure 13: Tibia Accelerometer Mount Attached with Gorilla Glue

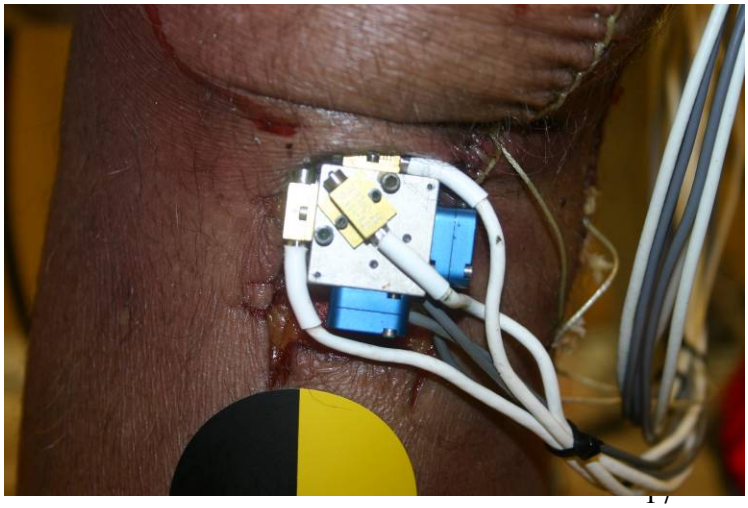

Figure 14: Tibia Accelerometer and Angular Rate Sensor Block

High speed video recorded each impact at 1000 frames per second. Using the video analysis software TEMA (Photo-Sonics International Ltd, Oxfordshire, UK) the angle of the tibia relative to the femur could be calculated. Because the video footage is limited to the YZ plane, only rotation about the x-axis could be obtained from the high speed footage. Due to this limitation, TEMA analysis was used to compare results with the 3aω blocks to verify the blocks' accuracy. For this reason, TEMA analysis is not presented in this report.

Section 5.2: **0901PED Specific Methods**

For the initial trial, a specific series of impacts were conducted on the right leg of subject 0901PED which can be found in Table 2. Because it was the first trial of its kind, a cautious test matrix was developed for subject 0901PED. In the initial test matrix, baseline impacts (Δh=4") were performed after each subsequent increase in height in order to compare the ligament response data for any change that would indicate injury. The voltage supply to the event trigger for trial 0901PED07R02 at the data acquisition system was turned off so an additional test at a height of seven inches (0901PED07R03) was performed. After reaching maximum height that the test rig would allow, (nineteen inches) a shoe with a 5 lb weight attached to it was put onto the foot to help increase the moment about the knee. This can be seen in Figure 15. The main goal of the initial trial was to verify that all instrumentation remained securely attached to the denuded leg while also determining an appropriate test matrix. Because of this and due to time restraints only the right leg of subject 0901PED was tested.

Table 2: 0901PED Test Matrix

Test Number	Height (in)	Corresponding Angle From Horizontal (Degrees)
0901PED04R01	4	-52
0901PED07R02	7	-40
0901PED08R03	7	-41
0901PED04R04	4	-52
0901PED10R05	10	-30
0901PED04R06	4	-51
0901PED14R07	14	-20
0901PED04R08	4	-51
0901PED19R09	19	-4
0901PED04R10	4	-51.5
0901PED19WR11	19 with 5 lb weight on foot	-4
0901PED04R12	4	-52

Figure 15: Shoe with 5 lb Weight Attached to Bottom of Foot

Section 5.3: 0902PED Specific Methods

Taking knowledge gleamed from the initial trial, a new test matrix was created for subject 0902PED and it can be found in Table 3. In this test series, three baseline impacts (Δh=4") were performed to pre-condition the leg and obtain an average for initial baseline response. It can also be noticed that for the left leg, a trial at a height of seven inches was not performed. Using data from the right leg it was determined that injury would not occur at a height of seven inches so in the interest of saving time the first height tested for the left leg after the baseline trials was ten inches. Like trial 0901PED, once the maximum height of nineteen

inches was reached and no injury was observed in the data traces, weight was added to the leg. In this test series, instead of adding a shoe with a 5 lb weight attached to it, a 2.5 lb ankle weight was attached to the leg as seen in Figure 16.

Table 3: 0902PED Test Matrix

Test Number Right Leg	Test Number Left Leg	*Height (in)	Corresponding Angle From Horizontal Right/Left (Degrees)
0902PED04R01	0902PED04L01	4	-54/-54
0902PED04R02	0902PED04L02	4	-54/-54
0902PED04R03	0902PED04L03	4	-54/-54
0902PED07R04	N/A	-	-41
0902PED10R05	0902PED10L04	10	-31/-32
0902PED14R06	0902PED14L05	14	-18/-19
0902PED19R07	0902PED19L06	19	-7/-6
0902PED19WR08	0902PED19WL07	19 with 2.5 lb ankle weights	-6/-7
0902PED04R09	0902PED04L08	4	-54/-54

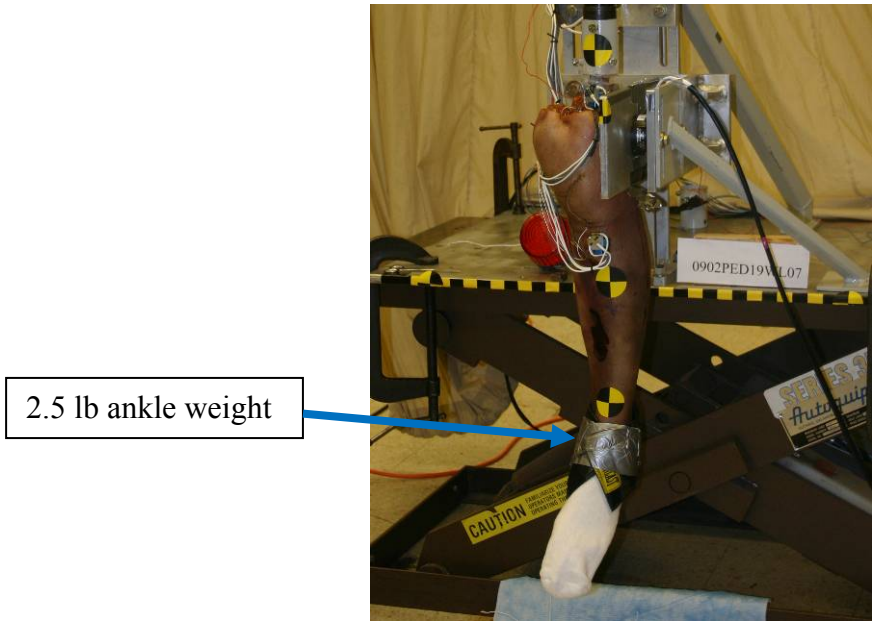

Figure 16: Leg with 2.5 lb Ankle Weight Attached

Section 5.4: 0903PED Specific Methods

A test matrix like that of trial 0902PED##L## was created for subject 0903PED and it may be found in Table 4. Again, this test series had three baseline impacts (Δh=4") performed to pre-condition the leg and obtain an average for an initial baseline response followed by an incremental increase in release height. Due to lack of subject availability, a third subject that was tested previously in the Injury Biomechanics Research Lab was used. From the previous test, all muscles of the thigh had been dissected at autopsy to look for possible injury to the femur. However, it should be noted that the subject's knee had not been tested in the previous study. Prior to the 0903PED test, due to the muscles being reflected from the femur, the knee joint was already compromised/lax in the medial/lateral direction, thus compromised lateral response during testing was expected as well. Despite this, the trial was performed as a way to verify instrumentation procedure, expecting data suggesting a compromised response, which was the ultimate goal of this research.

Table 4: 0903PED Test Matrix

Test Number	Height (in)	Corresponding Angle From Horizontal (Degrees)
0903PED04R01	4	-56
0903PED04R02	4	-56
0903PED04R03	4	-56
0903PED10R04	10	-34
0903PED14R05	14	-22
0903PED19R06	19	-7
0903PED04R07	4	-56
0903PED19WR08	19 with 2.5 lb ankle weights	-7
0903PED04R09	4	-56

Section 5.5 Data Processing

All signals were acquired using a 32-channel data acquisition system with a sampling rate of 20,000 Hz (Yokagowa Corporation of America). Each signal was zeroed and filtered according the specifications recommended by SAE J211. SAE J211 states the time should have a

resolution of at least 1/100 s [10] and recommends filtering according to Channel Frequency Class (CFC). The CFC can be converted to a low-pass Butterworth filter. Refer to Table 5 for the conversion of CFC to Butterworth filter.

Table 5: CFC to Low-Pass Butterworth Filter

CFC	Equivalent Butterworth Filter Frequency (Hz)
60	100
180	300
600	1000
1000	1650

SAE J211 states that the forces and moments applied to the leg are to be CFC 600, while accelerations are to be CFC 1000. Refer to Appendix G to view an example of the MATLAB script file used to process the data.

To ensure the measurements of motion of the tibia and femur were recorded in the global coordinate system of the subject, the accelerometer coordinate system was transformed into the global coordinate system. The global coordinate system was used under the assumption that for the short time at impact, where the femur is close to vertical, the global coordinate system is stationary. A list of all digitized points can be viewed in Appendix F.

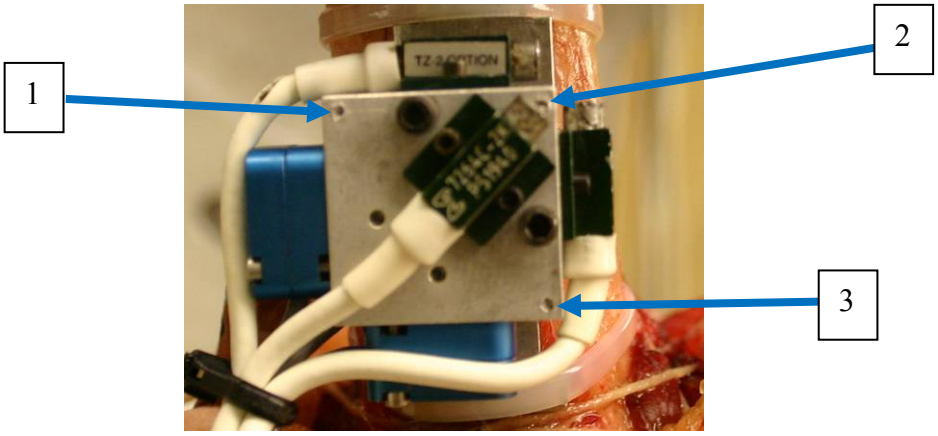

Figure 17: FARO Locations on Accelerometer Blocks

For both the femur and tibia accelerometer mounting blocks, three points were digitized, in a clockwise manor on the face of the accelerometer block, as shown in Figure 17 and in a schematic in Figure 18. The yellow dots in Figure 18 represent the three points recorded by the FARO Arm. The red arrows in Figure 18 represent the axis in which each accelerometer is recording.

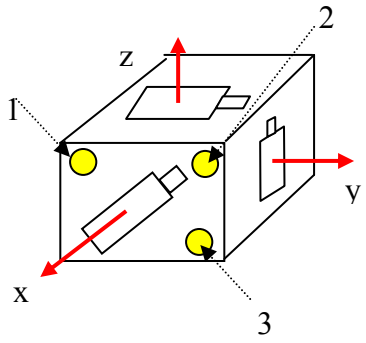

Figure 18: Accelerometer Block Point Digitization

Using the three points recorded on the block, two vectors and a cross were created to define the coordinate system of the accelerometer block. By knowing both the accelerometer block's coordinate system as well as the global coordinate system, the signals from each accelerometer block could be rotated into the global coordinate system. Refer to Appendix G to view the MATLAB script files that were used in this project.

CHAPTER 6

RESULTS

Section 6.1: 0901PED Results

The first subject tested 0901PED was a 91 year old male. Despite his age, the subject did not suffer from osteoporosis. The subject's anthropomorphic data is shown below in Table 6. Note that the test data was not normalized for each subject because the aim of this study is to evaluate instrumentation and not define injury criterion or determine the biomechanical properties of the lower extremities.

Table 6: 0901PED Subject Information

PMHS ID	Age	Leg	Stature (cm)	Cut Femur Length (cm)	Knee Circumference (cm)	Denuded Weight of Leg (N)
0901PED	91	Right	179	28	36	42
		Left		N/A	N/A	N/A

As was common on all subjects, the Micro-DVRTs that were used to measure ligament displacement were inserted near the center of each ligament. Because of this, the Micro-DVRT could only measure displacement on the portion where the Micro-DVRT was inserted. In order to get an estimate of the overall stretch for the entire ligament a scaling factor was used. It was assumed that the ligament displaced evenly across the entire length of the ligament. With this assumption a scaling factor with the ratio of ligament length to barb-to-barb distance was used. The ACL and MCL ligament lengths as well as the barb-to-barb distance of the Micro-DVRTs are shown in Table 7. The table also includes the scaling factor used and the DVRT serial number.

Table 7: 0901PED Ligament Information

PMHS ID	Leg	Ligament	Ligament Length (mm)	Barb Distance (mm)	Scaling Factor	DVRT Serial #
0901PED	Right	ACL	38	17	2.24	0001
		MCL	55	17	3.24	0003

The results from all impacts to the right leg are shown in Table 8. The table shows the maximum ACL and MCL stretch recorded for each impact. Test 0901PED19R09 (highlighted blue in the table) is believed to be when injury occurred to the ACL. Figure 19 and Figure 20 on the next pages will explain this further.

Table 8: 0901PED Initial Test Results

Baseline Trials
Injury Trial

Test Number:	Impact Height: (in)	ACL Stretch: (mm)	MCL Stretch: (mm)
0901PED04R01	4	0.52	2.10
0901PED07R02	7	N/A	N/A
0901PED07R03	7	0.89	2.58
0901PED04R04	4	0.43	2.49
0901PED10R05	10	1.28	3.47
0901PED04R06	4	0.51	2.68
0901PED14R07	14	1.59	4.33
0901PED04R08	4	0.53	2.60
0901PED19R09	19	1.81	4.81
0901PED04R10	4	1.29	3.48
0901PED19WR11	19 with 5lb weight	4.47	4.50
0901PED04R12	4	0.49	5.60

**** NOTE:** As can be seen above in the Table 8 trial 0901PED07R02 has no data available. For this trial, the data acquisition equipment did not trigger. For this reason, the same trial was re-run as 0901PED07R03 in order to obtain data for the given height.

Figure 19 shows the ACL stretch recorded during all lateral impacts to the right knee of subject 0901PED. Baseline impacts are represented as dashed lines with the same color as the impact seen previous it. The vertical dashed line shows the point where injury occurred. At this time, the ACL stretch recorded was 1.65 mm at a time of 49.25 ms during trial 0901PED19R09 where the leg was dropped from a height of 19". At this point it can be determined that fibers of the ACL began to tear, as its return response deviated from the path seen from previous impacts. This was verified by the following baseline test (0901PED04R10) in which the response was much different than that of all of the previous baseline tests as shown in Figure 19. This injury was not noticed at test time and an additional test was performed in which a 5 lb weight was added to the bottom of the foot (see Figure 15) and raised to the same height of 19". This curve is seen in Figure 19 as test 0901PED19WR11. This additional test was the likely cause of the complete tear of the ACL from the femur and the avulsion of the capsule from the medial tibia plateau. Notice that the during the following baseline test (0901PED04R12) no ACL stretch occurred, again suggesting that complete tear occurred during trial 0901PED19WR11.

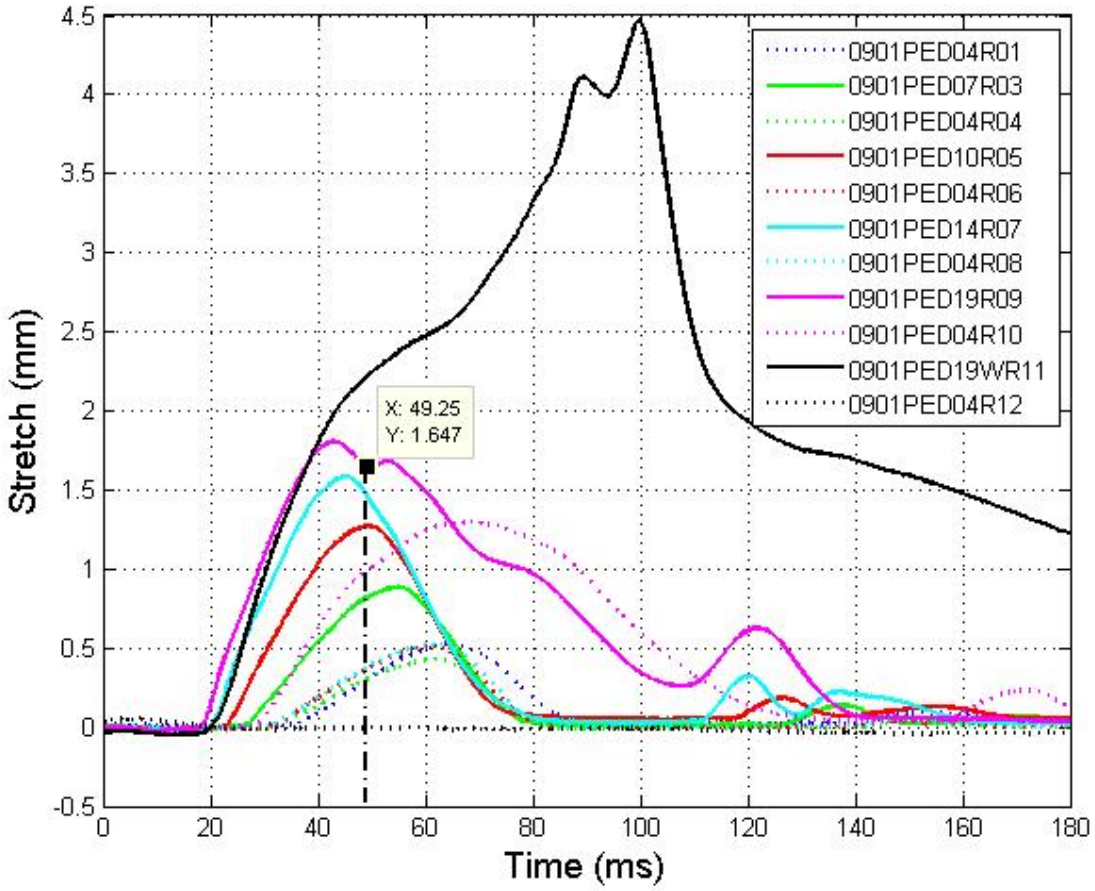

Figure 19: 0901PED ACL Stretch from Different Impact Heights with Time of Injury Labeled

Figure 20 shows the MCL stretch recorded during all lateral impacts to the knee. Just like Figure 19, baseline impacts are represented as dashed lines with the same color as the impact seen previous to it. The maximum MCL stretch recorded during the trial in which injury occurred to the ACL (0901PED19R09) is labeled on the plot. Its value is 4.81 mm and occurred at a time of 49.25 ms. Although no injury occurred to the MCL, it can be noticed that the baseline trial following injury to the ACL (0901PED04R10) shows much more stretch in the MCL than the previous trials, but still follows a similar return path. This is likely due to the increased loading to the MCL due to the ACL injury. It should also be noted that after the trial with the weight attached to the foot, it can be seen that in the following baseline trial

(0901PED04R12) the MCL stretch increases even more suggesting it sees more loading. This supports the conclusion that it was during trial 0901PED19WR11 that the complete tear of the ACL occurred.

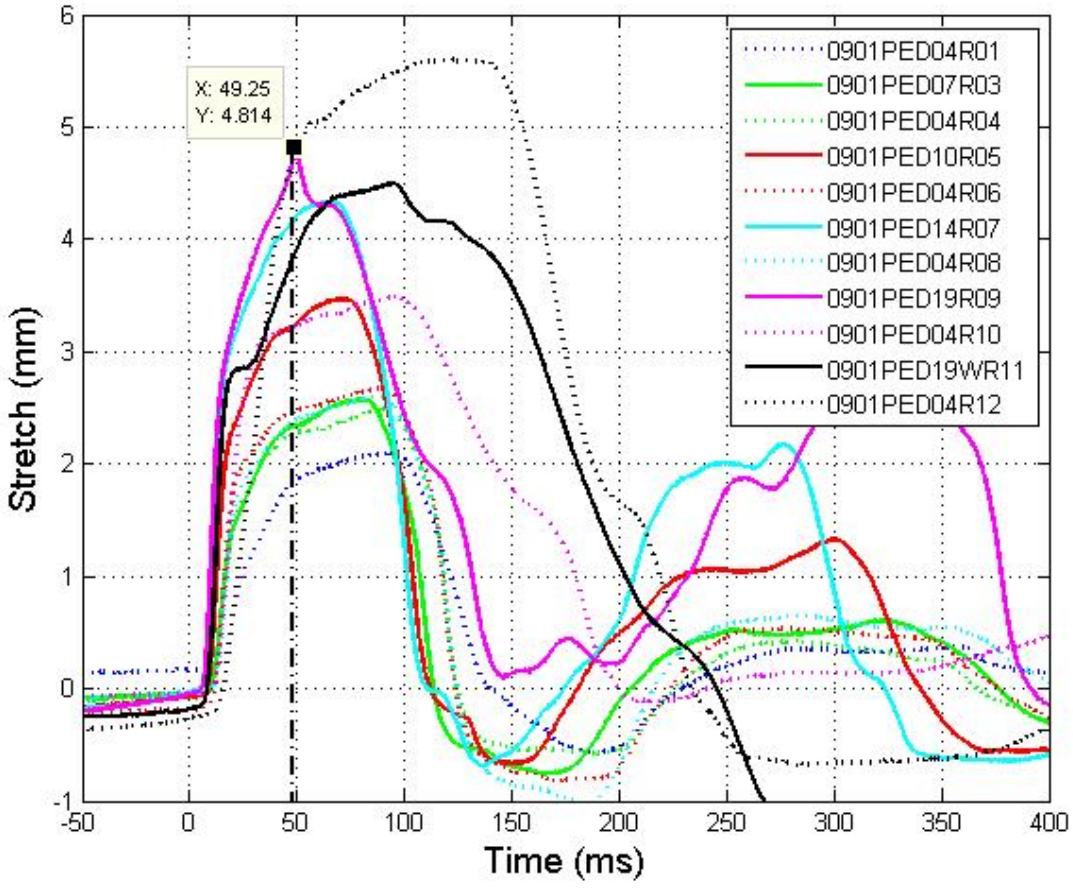

Figure 20: 0901PED MCL Stretch Data with Time of Injury Labeled

Figure 21 shows the angle of the tibia relative to the global coordinate system for trial 0901PED19R09 in which injury occurred to the knee. It reveals that a considerable amount of rotation occurs about both the x-axis and z-axis, with close to -17 degrees and 13 degrees rotation about each axis respectively. For all subjects tested, rotation about the y-axis is not presented as rotation about this axis expected in the normal range of motion of the knee joint, i.e. the extension and flexion seen in gait.

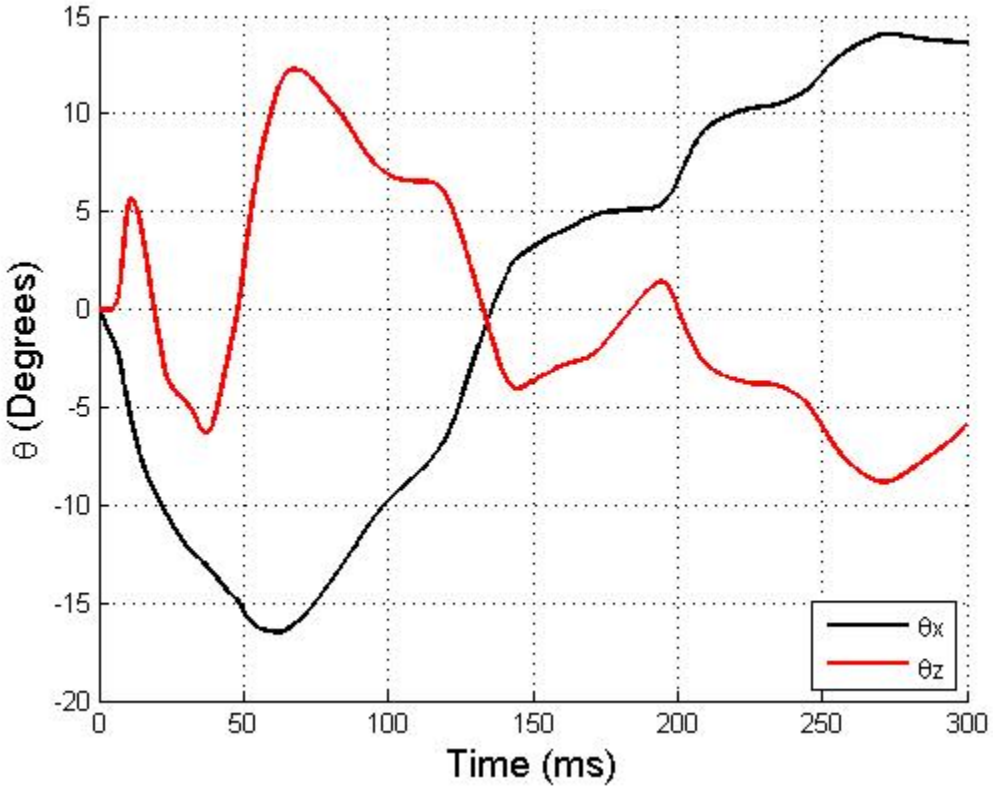

Figure 21: 0901PED Angular Rotation of Tibia about x and z-axis of GCS During Injury Trial

Figure 22 plots ACL and MCL stretch for trial 0901PED19R09 in which injury occurs. Along with the ligament stretch resultant angular velocity is also plotted on the right y-axis against time. It can be noticed that at time of injury there is also a spike in resultant angular velocity. This suggests that resultant angular velocity may be a candidate to be used as an indicator of injury.

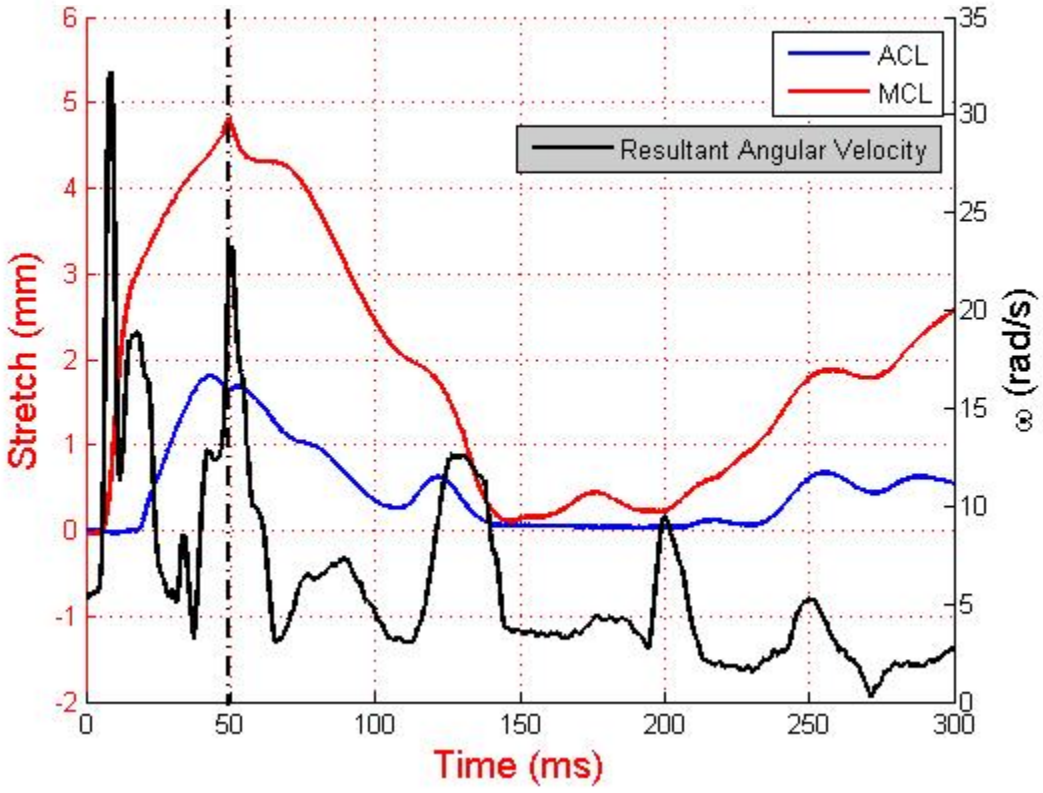

Figure 22: 0901PED ACL and MCL Stretch with Resultant Angular Velocity

Section 6.2: 0902PED Results

The second subject tested 0902PED was a 61 year old male and did not suffer from osteoporosis. The subject's anthropomorphic data is shown below in Table 9.

Table 9: 0902PED Subject Information

PMHS ID	Age	Leg	Stature (cm)	Cut Femur Length (cm)	Knee Circumference (cm)	Denuded Weight of Leg (N)
0902PED	61	Right	177.5	28	41	80
		Left		28	40	73

The ACL and MCL ligament lengths as well as the barb-to-barb distance of the Micro-DVRTs are shown below in Table 11. The table also includes the scaling factor used and the DVRT serial number. It should also be noted that on subject 0902PED the MCL was poorly

defined making attachment of the Micro-DVRT difficult. Because of this, results from the MCL stretch were unreliable. Table 10 below shows the variability the MCL had from subject to subject. Here it can be seen that subject 0902PED's MCL is poorly defined in comparison to subjects 0901PED and 0903PED.

Table 10: Comparison of Subject's MCLs

0901PED MCL	0902PED MCL	0903PEDMCL
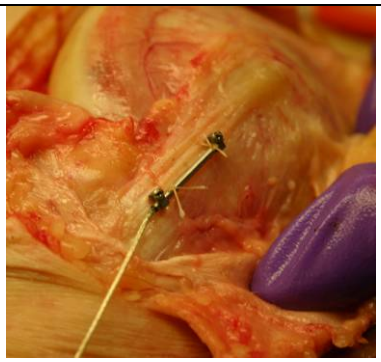	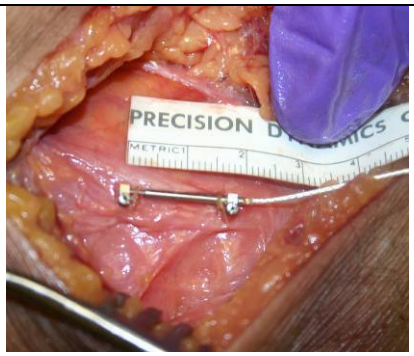	

Table 11: 0902PED Ligament Information

PMHS ID	Leg	Ligament	Ligament Length (mm)	Barb Distance (mm)	DVRT Serial #
0902PED	Right	ACL	32	15	0003
		MCL	55	18	0001
0902PED	Left	ACL	33	16	0006
		MCL	60	19	0004

The results from all impacts to the right and left leg are shown in Table 12. The table shows the maximum ACL and MCL stretch seen for each impact. The trials highlighted in yellow are the baseline trials and the trials highlight in blue are the trials in which injury occurred. Note that because of poor MCL definition in the subject, MCL data, especially on the left leg is unreliable.

Table 12: 0902PED Initial Test Results

Baseline Trials
Injury Trial

Test Number:	Impact Height: (in)	ACL Stretch: (mm)	MCL Stretch: (mm)
0902PED04R01	4	0.60	4.94
0902PED04R02	4	0.68	5.08
0902PED04R03	4	0.88	6.10
0902PED07R04	7	0.97	7.27
0902PED10R05	10	1.60	7.98
0902PED14R06	14	2.14	9.42
0902PED19R07	19	2.19	11.61
0902PED19WR08	19 with 5lb weight	2.52	12.86
0902PED04R09	4	1.05	11.07
Left Leg			
0902PED04L01	4	0.62	39.70
0902PED04L02	4	0.71	20.06
0902PED04L03	4	0.83	22.60
0902PED10L04	10	1.33	20.82
0902PED14L05	14	1.48	13.16
0902PED19L06	19	1.67	13.86
0902PED19WL07	19 with 5lb weight	1.68	4.66
0902PED04L08	4	0.67	4.13

Figure 23 shows the ACL stretch recorded during all lateral impacts to the right knee of subject 0902PED. All dashed lines show baseline trials. The vertical dashed line shows where it is believed point of injury occurred. At this time, the ACL stretch recorded was 2.41 mm at a time of 62.25 ms during trial 0902PED19WR08 where the leg was dropped from a height of 19" with a 2.5 lb ankle weight attached. At this point it can be determined that fibers of the ACL began to tear, as its return response deviated from the path recorded from previous impacts. This was verified by the following baseline test (0902PED04R09) in which the response was much different than that of all of the previous baseline tests as seen in Figure 23.

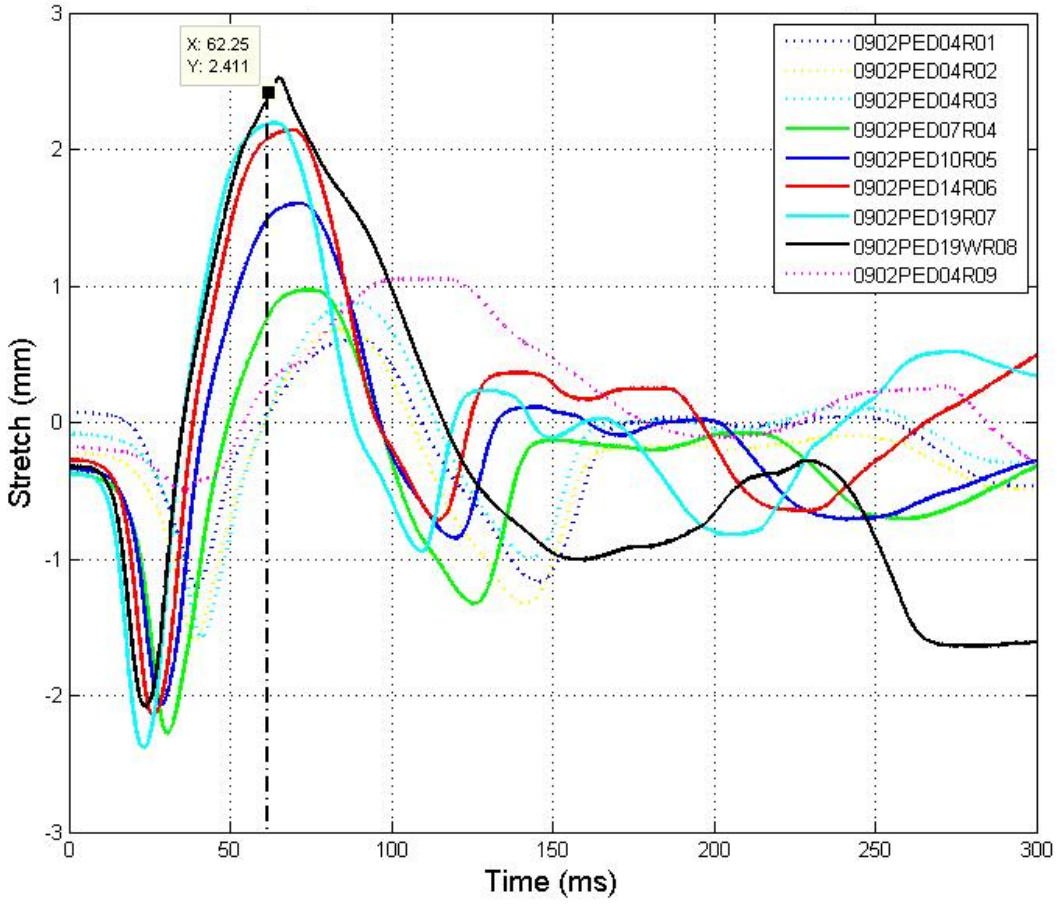

Figure 23: 0902PEDR ACL Stretch from Different Impact Heights with Time of Injury Labeled

Figure 24 shows the MCL stretch recorded during all lateral impacts to the right knee of subject 0902PED. The maximum MCL stretch recorded on the trial in which injury occurred to the ACL (0902PED19WR08) is labeled on the plot. Its value at time of injury is 12.61 mm and occurred at 62.25 ms. Although no injury occurred to the MCL, it can be noticed that the baseline trial following injury to the ACL (0902PED04R09) shows much more stretch in the MCL than previous baseline trials. Again, this is likely due to the increased loading to the MCL due to the ACL injury.

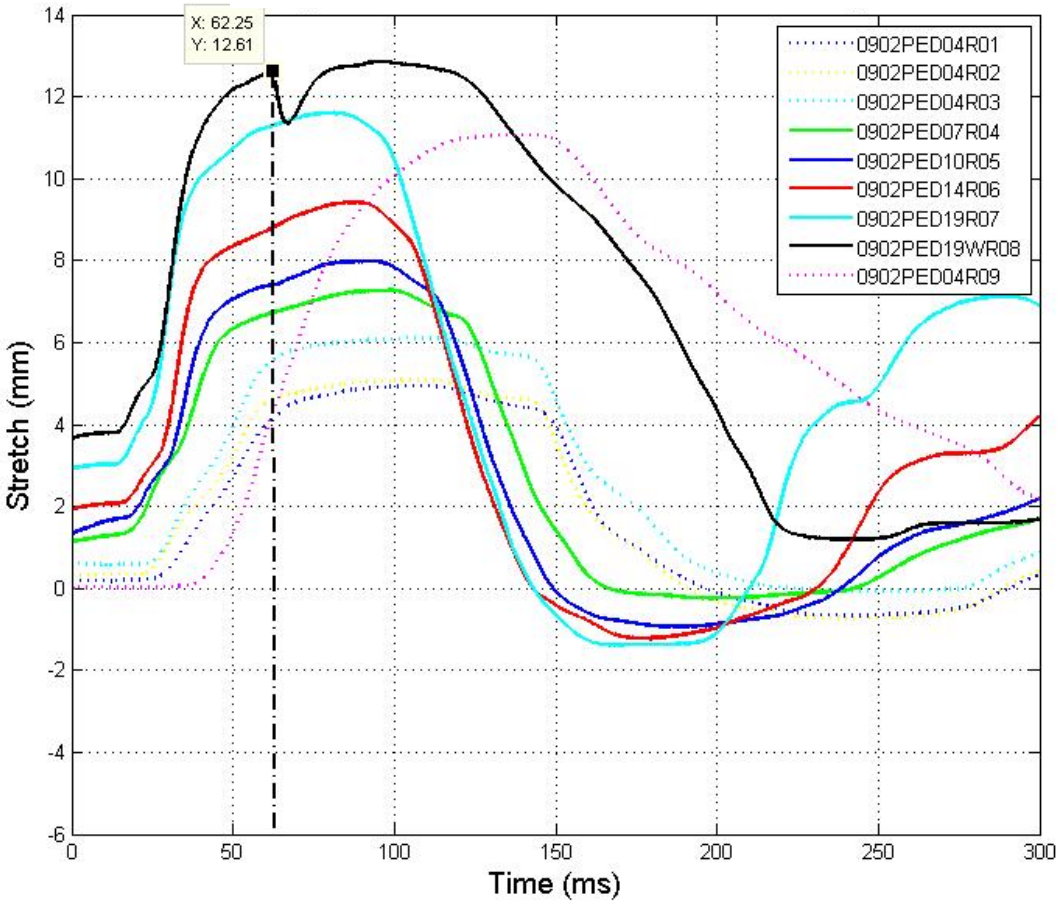

Figure 24: 0902PEDR MCL Stretch from Different Impact Heights with Time of Injury Labeled

Figure 25 shows the angle of the tibia relative to the global coordinate system for trial 0902PED19WR08 in which injury occurred to the knee. It shows a considerable amount of rotation occurs about both the x-axis and z-axis, with close to -22 degrees and 30 degrees rotation about each axis respectively.

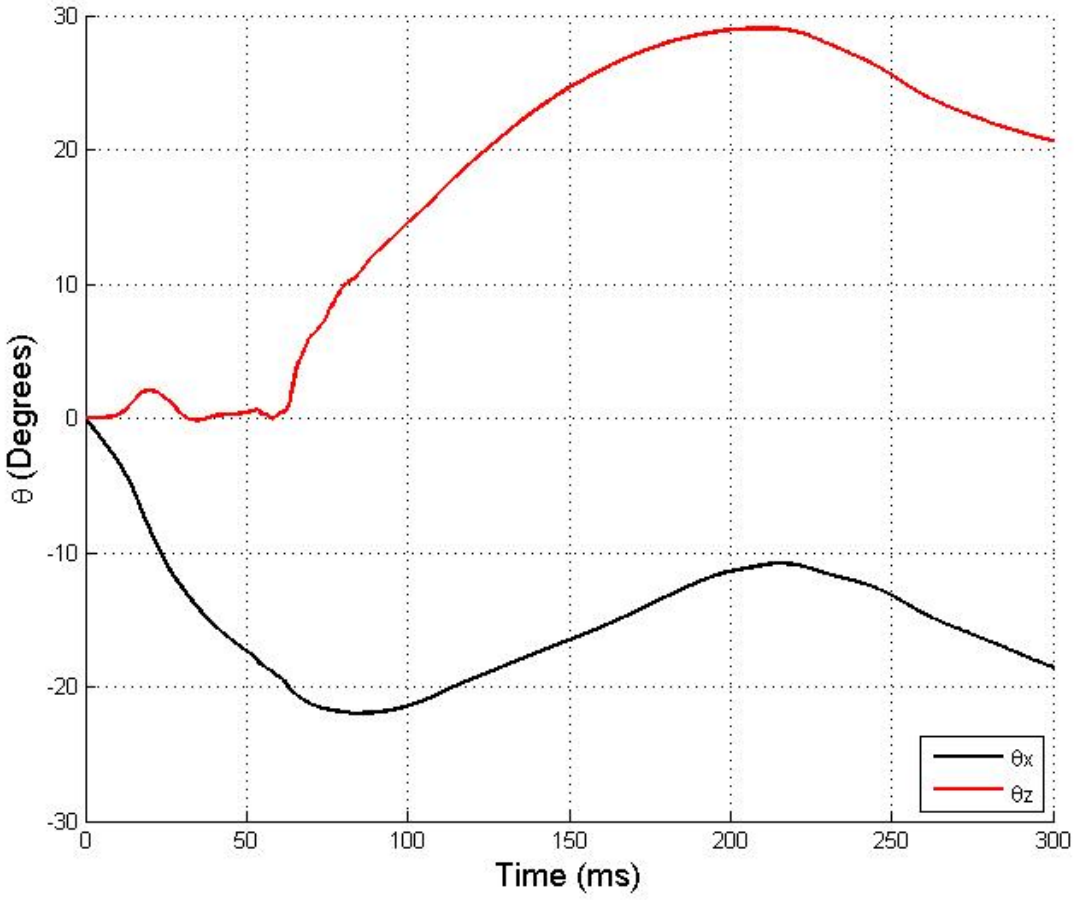

Figure 25: 0902PEDR Angular Rotation of Tibia about x and z-axis of GCS

Figure 26 plots ACL and MCL stretch for trial 0902PED19WR08 in which injury occurs. Along with the ligament stretch resultant angular velocity is also plotted on the right y-axis against time. Just like in trial 0901PED19R09, it can be noticed that at time of injury there is also a spike in resultant angular velocity. This supports the hypothesis that resultant angular velocity may be a candidate as an indicator of injury.

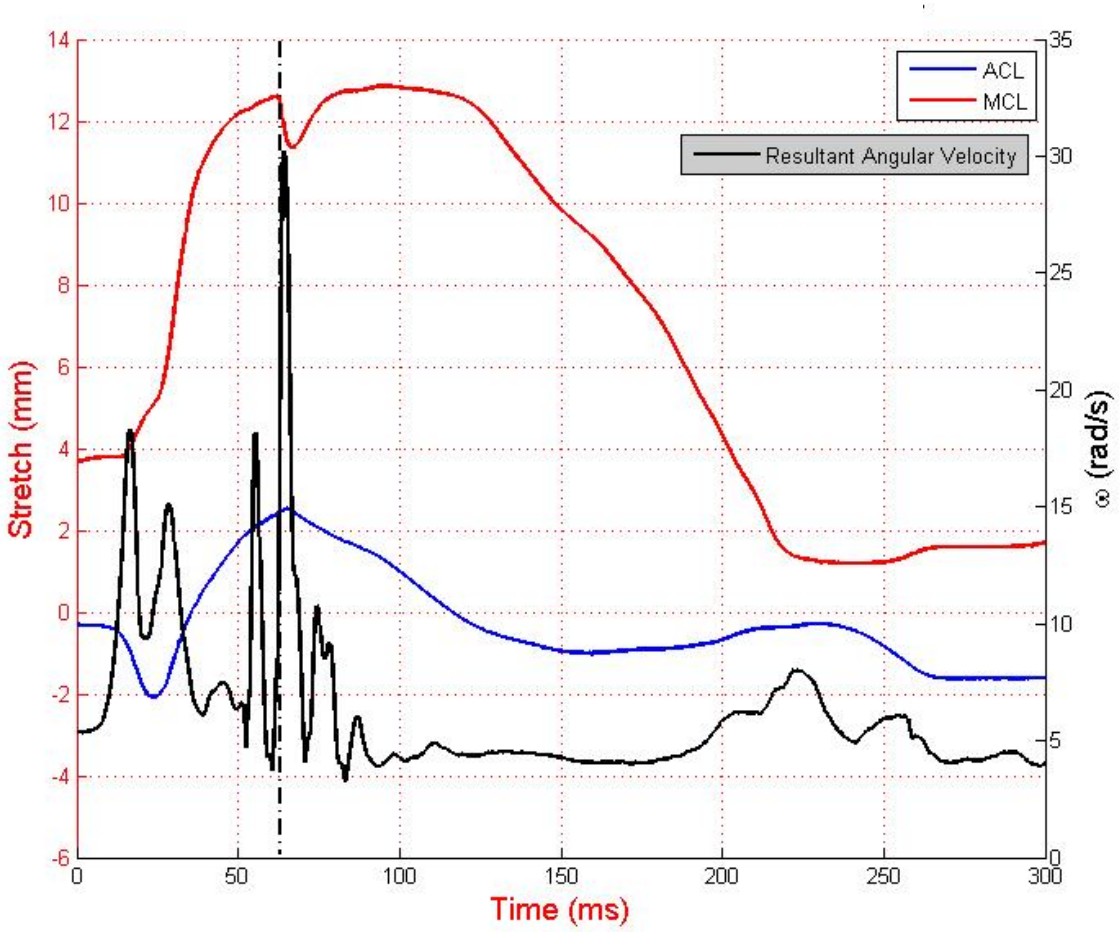

Figure 26: 0902PEDR ACL and MCL Stretch with Resultant Angular Velocity

Figure 27 shows the ACL stretch recorded during all lateral impacts to the left knee of subject 0902PED. All dashed lines show baseline trials. The vertical dashed line shows where estimated point of injury occurred. Because MCL data was compromised it was hard to identify an exact time for injury. However, at this assumed time, the ACL stretch recorded was 1.54 mm at a time of 57.6 ms during trial 0902PED19WL07 where the leg was dropped from a height of 19" with a 2.5 lb ankle weight attached. It appears that fibers of the ACL began to tear, as its return response deviated from the path recorded from the previous impacts. This again was

verified by the following baseline test (0902PED04L08) in which the response was much different than that of all of the previous baseline tests as shown in Figure 27.

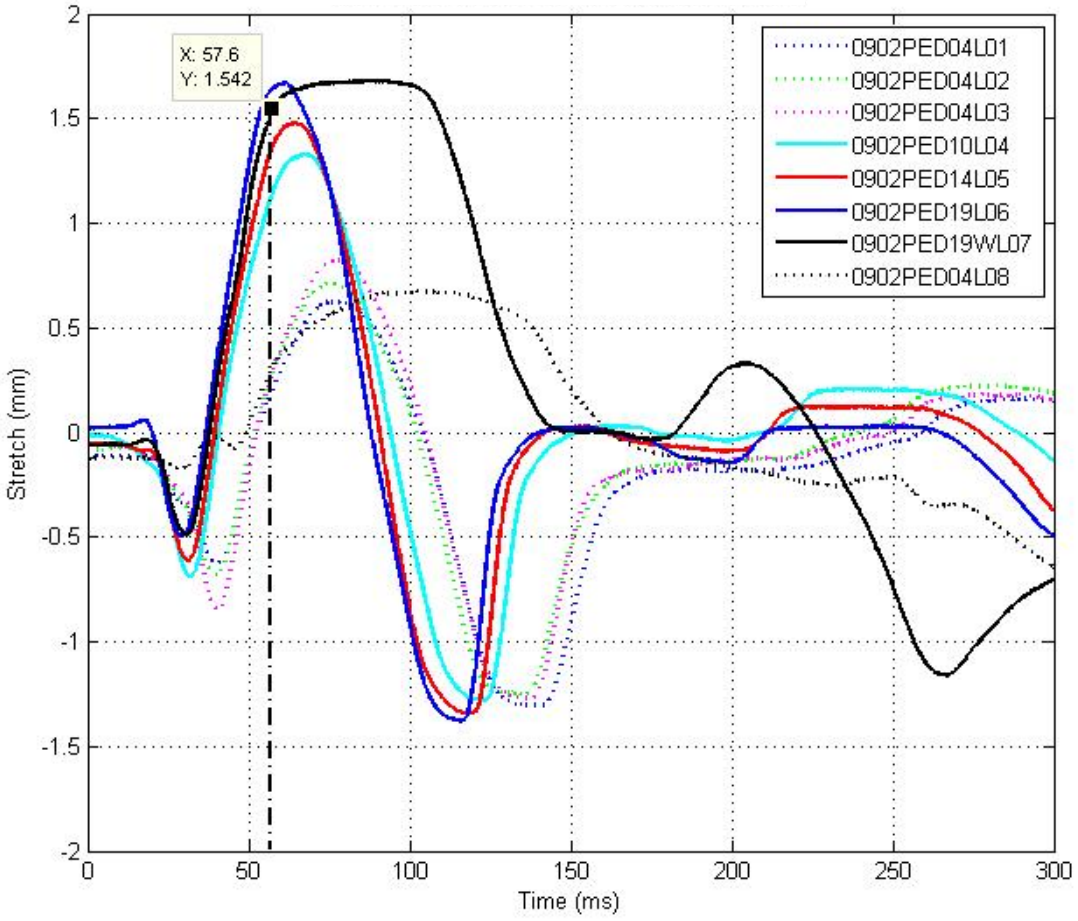

Figure 27: 0902PEDL ACL Stretch from Different Impact Heights with Time of Injury Labeled

Figure 28 shows the MCL stretch recorded during all lateral impacts to the left knee of subject 0902PED. From the plot it can be seen that with a poorly defined MCL, reliable data from the Micro-DVRT is difficult to obtain. At autopsy it was confirmed that the DVRT was still sutured in place, but the proximal DVRT slid into tissue lateral to the MCL and thus was not

perpendicular and did not move properly with the ligament. As a result unreliable data was obtained and appears in Figure 28.

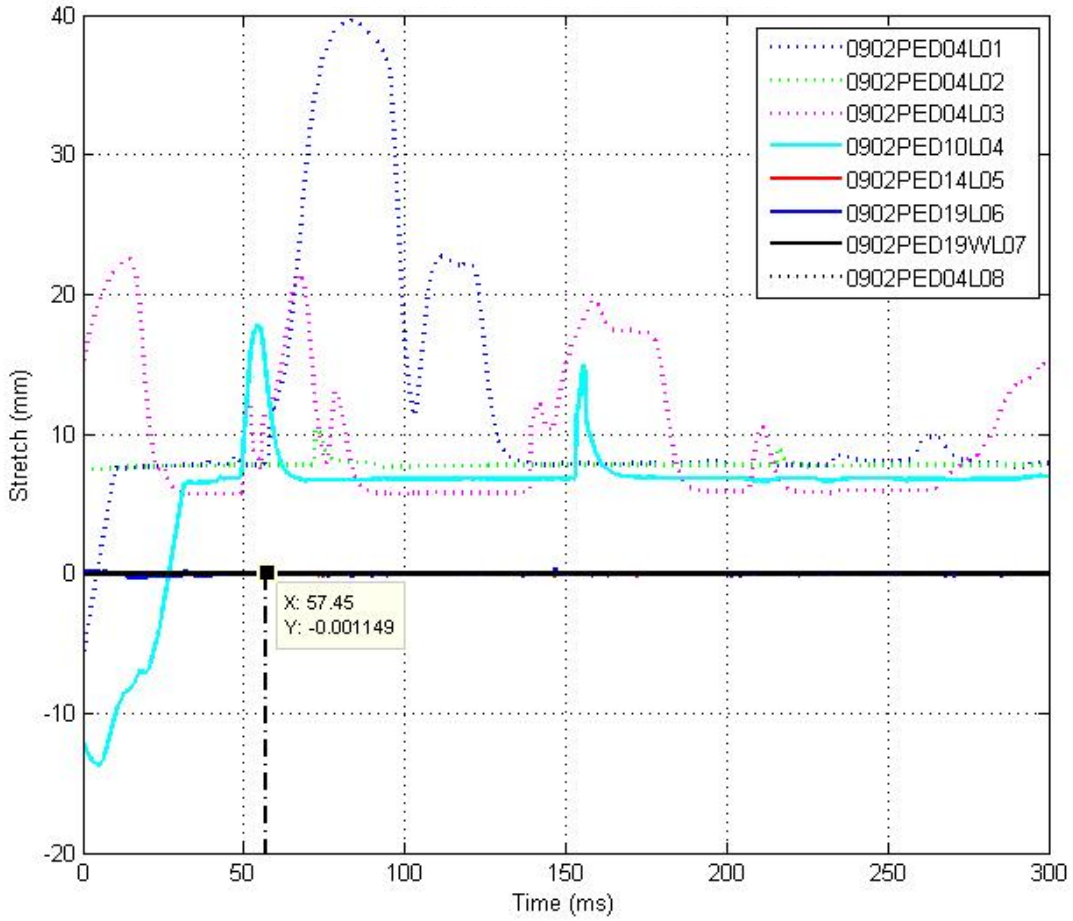

Figure 28: 0902PEDR MCL Stretch from Different Impact Heights with Time of Injury Labeled

Figure 29 shows the angle of the tibia relative to the global coordinate system for trial 0902PED19WL07 in which injury occurred to the knee. It can be seen that a considerable amount of rotation occurs about both the x-axis and z-axis, with close to 23 degrees and -14 degrees rotation about each axis respectively.

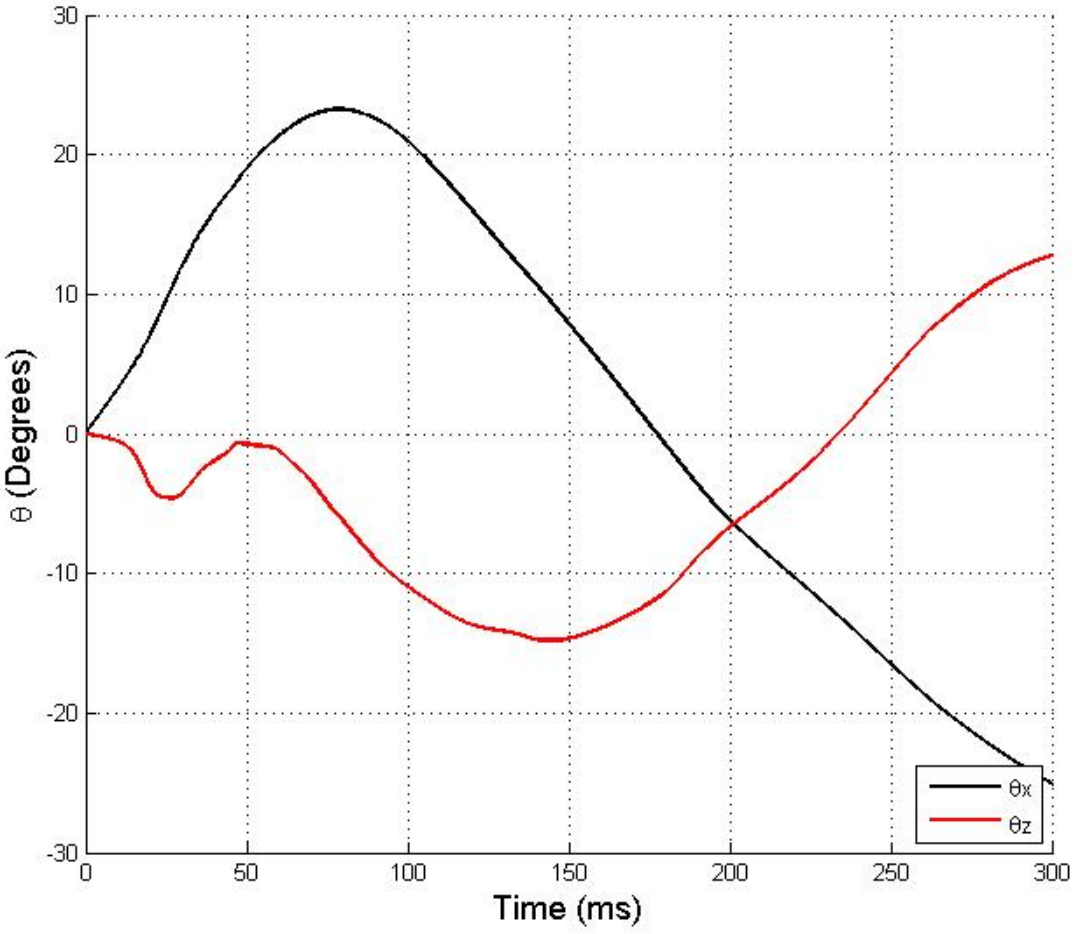

Figure 29: 0902PEDL Angular Rotation of Tibia about x and z-axis of GCS

Figure 30 plots ACL and MCL stretch for trial 0902PED19WL07 in which injury occurs. Along with the ligament stretch resultant angular velocity is also plotted on the right y-axis against time. Just like in the previous trials, it can be noticed that at estimated time of injury there is also a spike in resultant angular velocity.

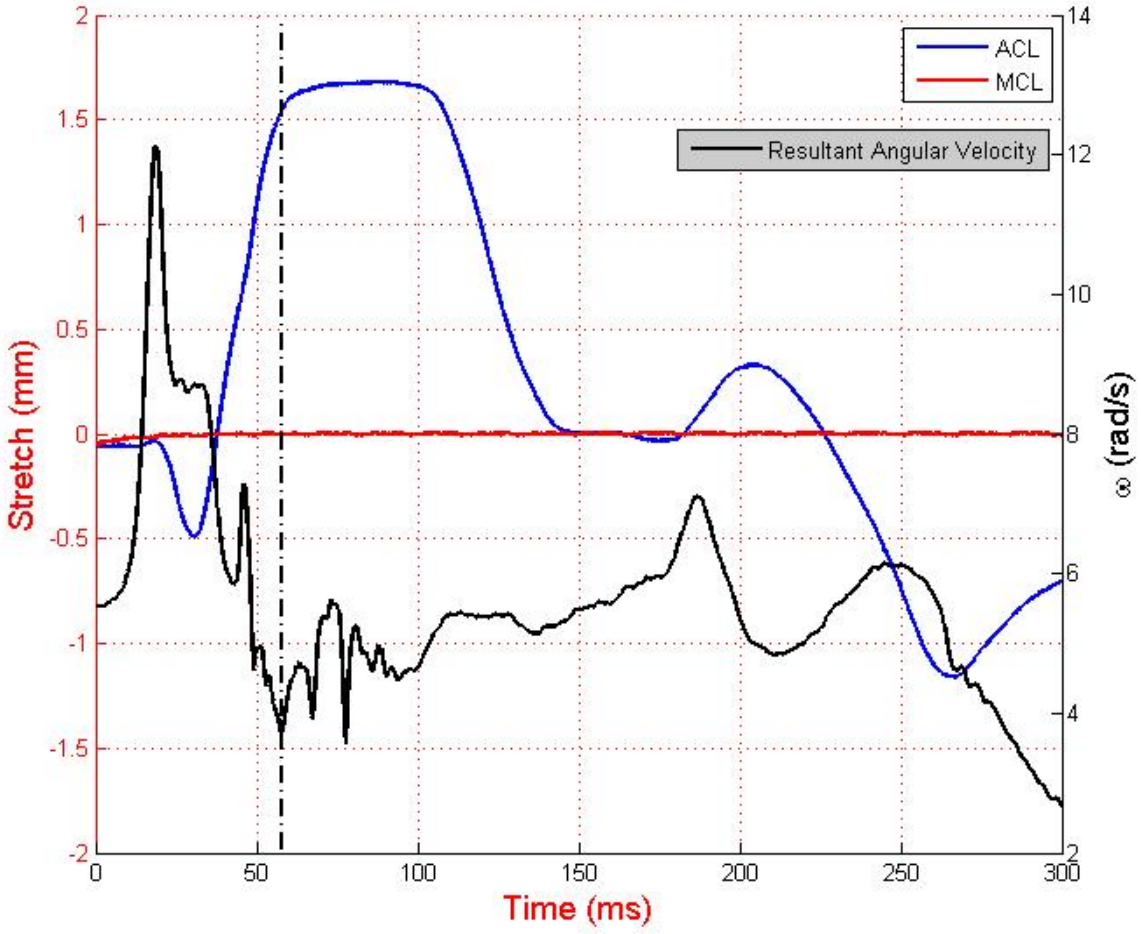

Figure 30: 0902PEDL ACL and MCL Stretch with Resultant Angular Velocity

Section 6.3: 0903PED Results

The third subject tested 0903PED was a 71 year old non-osteoporotic male. The subject's anthropomorphic data is shown below in Table 13.

Table 13: 0903PED Subject Information

PMHS ID	Age	Leg	Stature (cm)	Cut Femur Length (cm)	Knee Circumference (cm)	Denuded Weight of Leg (N)
0903PED	71	Right	171	28	41	73

The ACL and MCL ligament lengths as well as the barb-to-barb distance of the Micro-DVRTs are shown below in Table 14. The table also includes the scaling factor used and the DVRT serial number.

Table 14: 0903PED Ligament Information

PMHS ID	Leg	Ligament	Ligament Length (mm)	Barb Distance (mm)	DVRT Serial #
0903PED	Right	ACL	33	18	0003
		MCL	57	18	0001

The results from all impacts to the right and left leg are shown in Table 15. The table shows the maximum ACL and MCL stretch seen for each impact. The trials highlighted in yellow are the baseline trials. For this subject, no ligament injury to the knee was obtained. Due to prior dissection of the muscles of the thigh, the knee joint was already compromised/lax in the medial/lateral direction, thus compromised lateral response during testing was expected as well.

Table 15: 0902PED Initial Test Results

Baseline Trials

Test Number:	Impact Height: (in)	ACL Stretch: (mm)	MCL Stretch: (mm)
0903PED04R01	4	0.59	2.54
0903PED04R02	4	0.62	2.46
0903PED04R03	4	0.64	2.29
0903PED10R04	10	1.07	3.14
0903PED14R05	14	1.09	3.74
0903PED19R06	19	1.72	5.25
0903PED04R07	4	0.61	2.29
0903PED19WR08	19 with 5lb weight	1.92	3.37
0903PED04R09	4	0.79	2.22

Figure 31 shows the ACL stretch recorded during all lateral impacts to the right knee of subject 0903PED. All dashed lines show baseline trials. It can be noticed that the ACL response

in Figure 31 is much different when compared to the response seen in subjects 0901PED and 0902PED. This was expected due to the prior dissection of the thigh muscles. As a result, the data should not be used for comparison in analysis for biomechanical response of the knee. Despite this, the figure still supports that the instrumentation developed for the ACL stretch works properly. During the test, no injury was noticed as the baseline trial (0903PED04R09) following the impact with a 2.5 lb ankle weight attached (0903PED19WR08) had a similar response to previous baseline impacts. This was confirmed at autopsy where no ligament injury was found.

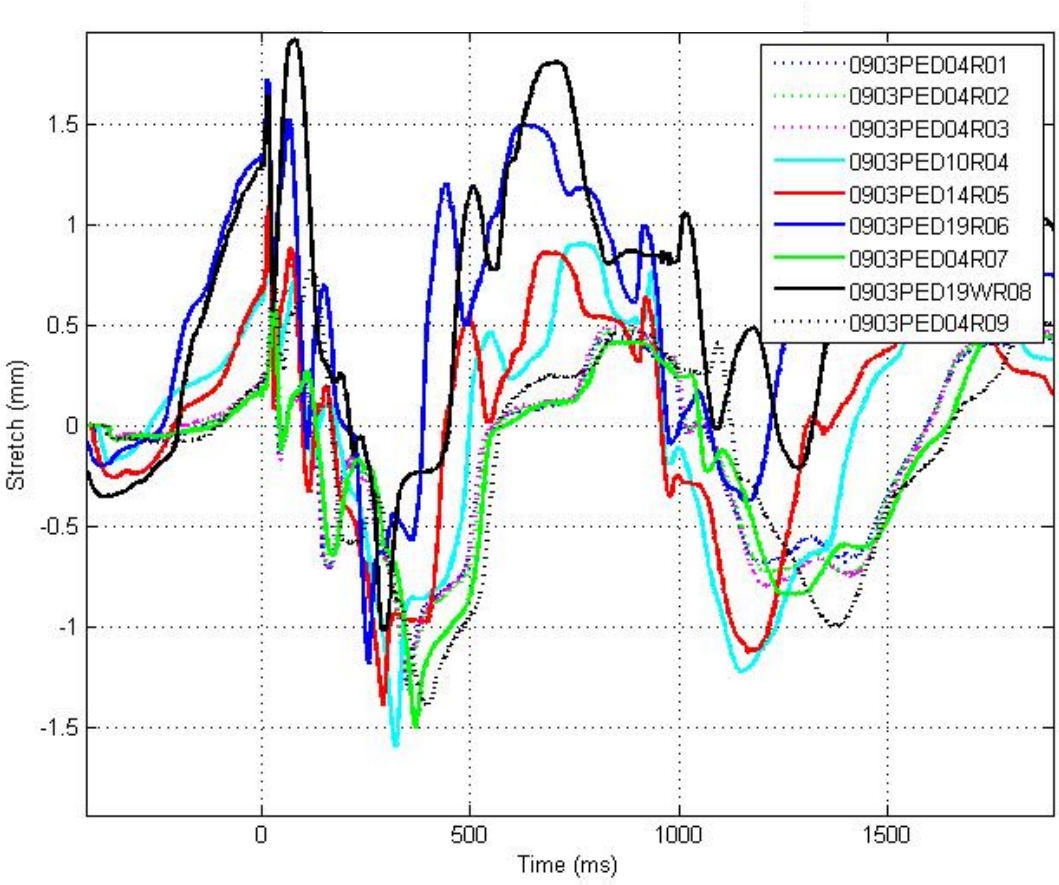

Figure 31: 0903PED ACL Stretch from Different Impact Heights

Figure 32 shows the MCL stretch recorded during all lateral impacts to the right knee of subject 0903PED. All dashed lines show baseline trials. Similar to the ACL data, MCL response was expected to vary for prior subjects.

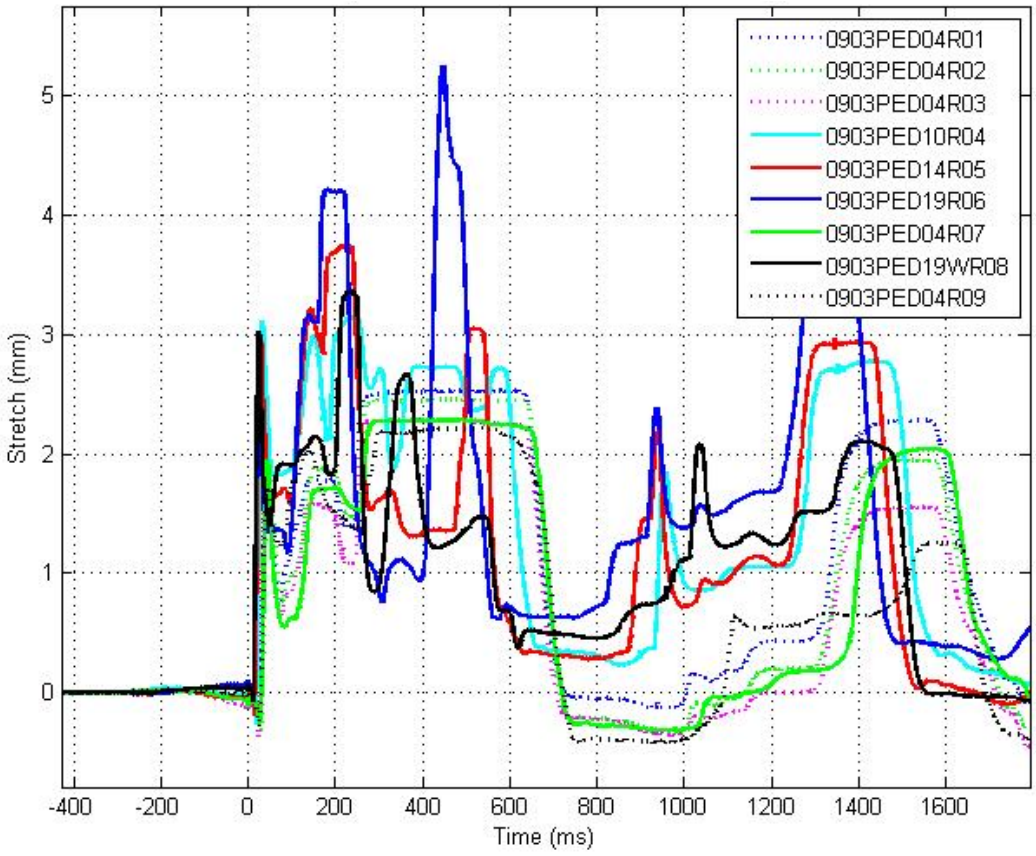

Figure 32: 0903PED MCL Stretch from Different Impact Heights

Figure 33 shows the angle of the tibia relative to the global coordinate system for trial 0903PED19WR08. It can be seen that a considerable amount of rotation occurs about both the x-axis and z-axis, with close to 33 degrees and 32 degrees rotation about each axis respectively. This rotation plot is also much different from that of subjects 0901PED and 0902PED. The increase in angular rotation can again be attributed to the pre-existing laxity in the knee due to

prior thigh muscle dissection. Again, rotation about the y-axis is not presented as rotation about this axis expected in the normal range of motion of the knee joint.

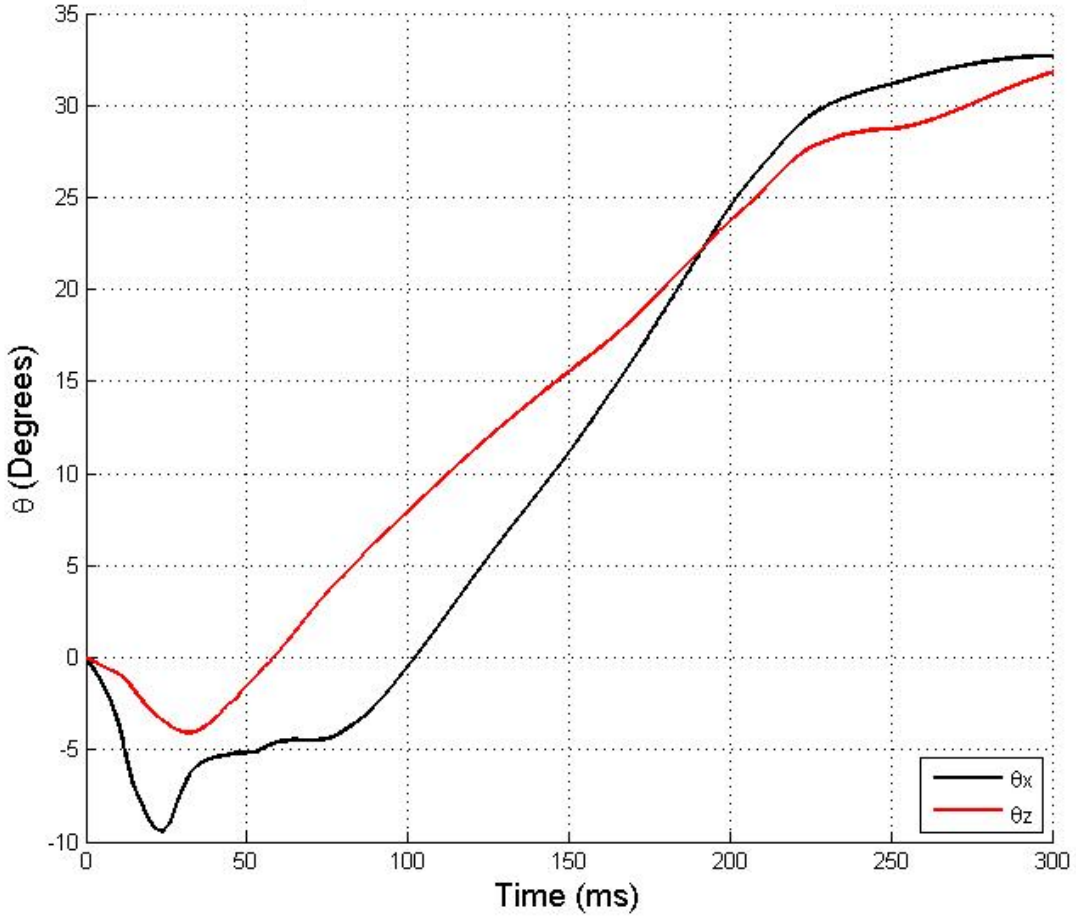

Figure 33: 0903PED Angular Rotation of Tibia about x and z-axis of GCS

Section 6.4: Summary of Results

Table 16 summarizes all injury information that was detected at autopsy. Listed in the table is the test number in which injury occurred, estimated time of injury, and a description of the type of injury that was documented.

Table 16: Summary of Injury Results

Test Number:	Time of Injury (TOI) (ms)	Injury
0901PED19R09	49.3	Tearing of ACL fibers
0901PED19WR09	N/A	ACL pure tear of 75% of the fibers. Small avulsion of the capsule off of the medial tibial plateau
0902PED19WR08	62.3	MCL- approx. 1/3 of fibers torn ACL- approx. 10% of fibers torn
0902PED19WL07	57.6	ACL- approx. 20-25% of ligament avulsed from femur
0903PED19WR08	N/A	No ligament injury found. Knee laxity was caused by prior dissection of thigh muscles

Figure 34 plots the ACL stretch for all trials in which initial injury occurred. For all trials where injury occurred to the ACL, the ACL stretch that was recorded at time of injury was between 1.5mm and 2.4mm.

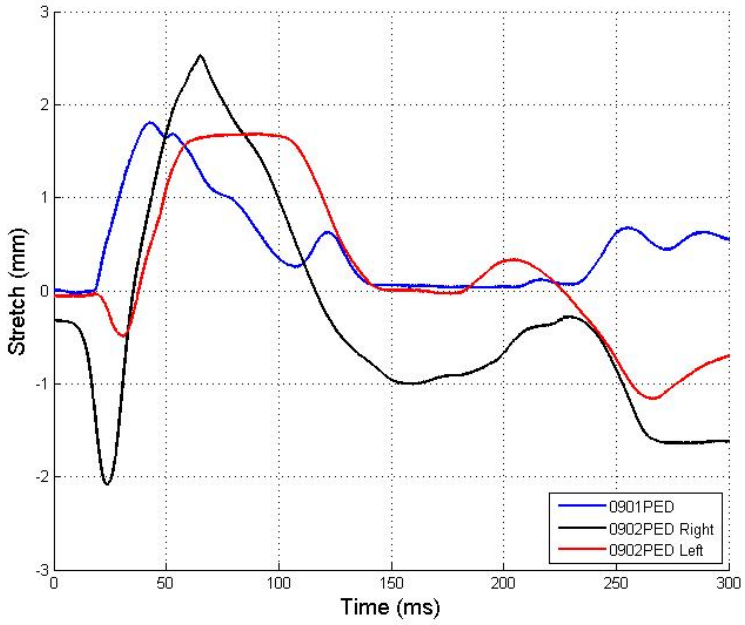

Figure 34: ACL Stretch seen on Injury Trials

CHAPTER 7

DISSCUSION

As shown in Table 16, the most common injury obtained during the lateral impacts to the knee was injury to the ACL. In trials in which injury occurred, at least partial tearing of some ACL fibers occurred in all subjects. This is supported by data from the angular rate sensors which show that both bending and twisting is occurring in the knee joint. It has been shown that a combination of twisting and bending is the most common cause for ACL injury. Although MCL injury was not common in the impacts, the MCL data acquired from the Micro-DVRT placed in the MCL aided in determining the time of injury for the ACL.

Instrumentation of the leg with accelerometers and angular rate sensors on the femur and tibia allowed for the motion of the leg to be captured for each impact of the leg. By attaching the blocks with wire ties and gorilla glue, compromising of the structural integrity of the bone was minimal. By having the angular rate sensors on the femur and tibia, the relative angular rotation between the tibia and femur could be determined during each impact. Having this information is vital in the understanding of what type of motion is occurring in the knee as well as helping explain why certain injuries occur. During the data analysis, it was noticed that at time of injury there was a correlation between resultant angular velocity and ligament injury. Only having three trials in which injury occurred, more trials and data are necessary to help support this relationship.

Although it is not presented in this thesis, load cell data along with the accelerometer and angular rate sensors could allow for analysis on the loading seen on the knee joint. This data

could be used to find the moment at the knee joint as well as the amount of shear forces that are acting on the knee joint.

With the instrumentation used in this paper, the time of injury for ACL and MCL failures can be determined along with ACL and MCL stretch at that time. Now that time of ACL and MCL injury can be determined, the next step in this research is to perform more trials to obtain potential injury criterion for the ligaments. With more trials, an estimation of maximum ligament stretch before injury could be estimated. More trials would also provide testing of the hypothesis that could either confirm or reject that resultant angular velocity and ligament injury have a correlation. With this instrumentation, a more real-world testing rig could be created to provide more realistic loading to the knee that is typical of pedestrian-vehicle collision or typical of common loadings documented in sports injuries.

CHAPTER 8

CONCLUSION

- Suturing the DVRT barbs to the ACL provided repeatable ACL displacement measurements

- When MCL is well defined, suturing the DVRT barbs to the MCL provided repeatable MCL displacement measurements

- The time of injury can be determined accurately with both MCL and ACL DVRT signals

- Angular velocity may be a predictor of injury that could be used in future work if more trials support this hypothesis

REFERENCES

1. Fleming BC, Beynnon BD. (2004). In vivo measurement of ligament/tendon strains and forces: a review. Annals of Biomedical Engineering. 32(3): 318-28.

2. van Dommelen JA, Jolandan MM, Invarsson BJ, Millington SA, Raut M, Kerrigan JR, Crandall JR, Diduch DR. (2005). Pedestrian injuries: viscoelastic properties of human knee ligaments at high loading rates. Traffic Injury Prevention. 6(3): 278-87.

3. Matsui Y. (2005). Effects of vehicle bumper height and impact velocity on type of lower extremity injury in vehicle-pedestrian accidents. Accident; analysis and prevention. 37(4): 633-40.

4. Otte D, Haasper C. (2007). Characteristics on fractures of tibia and fibula in car impacts to pedestrians and bicyclists - influences of car bumper height and shape. Annual Proceedings/ Association for the Advancement of Automobile Medicine. 51:63-67.

5. Untaroiu C, Kerrigan J, Kam C, Crandall J, Yamazaki K, Fukuyama K, Kamiji K, Yasuki T, Funk J. (2007). Correlation of strain and loads measured in the long bones with observed kinematics of the lower limb during vehicle-pedestrian impacts. Stapp Car Crash Journal. 51:433-66.

6. Pfefferle K.J., McFadden J, Donnelly B, Herriott R, Bolte J. (2006). Design and Evaluation of Measurement Instrumentation Used For High Energy Impacts on Fresh Post-Mortem Human Subjects. The Ohio State University.

7. Mallory A., Stammen J., TRC and NHTSA VRTC. Lower Extremity Pedestrian Injury in the U.S.: A Summary of PCDS Data, AB note 06-01.

8. Kajzer et al. (1997). Shearing and Bending Effects at the Knee Joint at High Speed Lateral Loading. Society of Automotive Engineers.

9. The American Journal of Sports Medicine. June 2008.

10. SAE Publication, SAE J211 – Instrumentation for Impact Test, SAE, 400 Commonwealth Drive, Warrendale, PA 15096-0001

11. The Netter Presenter: Human Anatomy Collection Version 2.0, Icon Learning System, LLC, Teterboro, NJ

12. Gavrila, D., DaimlerChrysler Research. Sensor-Based Pedestrian Protection. Intelligent Transportation Systems, 77-81.

13. Schwoerer, M. The Truth About Europe's Pedestrian Safety Legislation. 13 Dec 2007. http://www.thetruthaboutcars.com/the-truth-about-europes-pedestrian-safety-legislation.

14. Bose et al. (2004). Injury Tolerance and Moment Response of the Knee Joint to Combined Valgus Bending and Shear Loading. Journal of Biomechanical Engineering, Vol. 130.

15. Zander et al. (2007). Prediction of Lower Extremity Injury Risks During an Impact on Modern Car Fronts with a Flexible Pedestrian Legform Impactor and the Pedestrian Legform Impactor According to EEVC WG 17. Paper Number 07-0206.

APPENDIX

A. Pretest Data Protocol

Pre-Test Data Protocol

Pre-Test Information:

Test Number: _____

Sex: □ Male __ Female Age: __ Weight: ___**kg** Height: ___**cm** Race: _____

Cause of Death: _____

Cadaver Appearance: _____

Anomalies: _____

Pre-Test Anthropometric Measurements	Right	Left
ALL MEASUREMENTS IN cm		
POSTERIOR DRAWER TEST (Firm or Mushy Endpoint)		
1. STATUR (Stature)		
2. FEMLNG (Femur Length)		
3. FEMDIA (Femur Diameter)		
4. LTGHCR (Lower Thigh Circumference)		
5. KNEECR (Knee Circumference)		
6. QUADCR (Quadriceps Circumference)		
7. CALFCR (Calf Circumference)		
8. ANKLCR (Ankle Circumference)		
9. DENWHT (Denuded Weight-Without Shoe-lbs.)		

Note: Measurements taken with Faro arm will be taken after leg has been potted (see faro arm measurement sheet)

1. Measured from crown of head to calcaneus.
2. Measured from denuded portion to proximal medial margin of tibia.
3. Denuded Portion, measured approximately 7" proximal to femoral condyles perpendicular to longitudinal (Z) axis of thigh-average of two cross sections.
4. Measured just superior to patella, perpendicular to longitudinal (Z) axis of thigh.
5. Measured with leg extended across mid-patella and antecubital crease.
6. Measured at portion of thigh where denuded bone ends perpendicular to longitudinal (Z) axis of thigh (approximately 7" Proximal to Femoral Condyles.)
7. Measures maximum circumference of the calf perpendicular to longitudinal (Z) axis of tibia.
8. Measured just superior to malleoli perpendicular to longitudinal (Z) axis of tibia.
9. Weight of leg without shoe-step on scale and tare weight, then add leg and record.

****All parameters and abbreviations taken from NHTSA Test Reference Guide Version 5, Volume II: Biomechanical Tests, May 2001.**

Pre Test Positioning Measurements	Right	Left
ACL Length (From Origin to Insertion)		
DVRT Barb Distance (Between Each Barb-Inserted)		
MCL Length (From Origin to Insertion)		
DVRT Barb Distance (Between Each Barb-Inserted)		
Serial Numbers for ACL and MCL DVRT	ACL: MCL:	ACL: MCL:

B. Pre-Test/Autopsy Examination Sheet

Lateral Tibia Impact Research

PRE-TEST EXAMINATION/AUTOPSY REPORT

Test Number:_____
Date of Death:_____
Cause of Death:_____
Test Date:_____
Specimen Leg: Right_____ Left_____

PRE-TEST EXAMINATION

Skin:

	Right	Left
Scars		
Cuts/Abrasions		
Bruises		
Other		

Joint Stability:

Knee Laxity (Firm or Mushy-Determined via physical manipulation)		
	Pre-Test-Right	**Pre-Test-Left**
Posterior:		
Medial/Lateral:		

POST-TEST (At Autopsy)

Joint Stability:

Knee Laxity (Firm or Mushy-Determined via physical manipulation)		
	Post-Test-Right	**Post-Test-Left**
Posterior:		
Medial/Lateral:		

Skin/Subcutaneous tissue/Muscle NFS (Not Further Specified):

Injured Area	**AIS Code**	**Right**	**Left**
Skin/Subcutaneous tissue/Muscle NFS	890099.1		
Abrasion	890202.1		
Contusion (hematoma)	890402.1		
Laceration NFS	890600.1		
Minor (superficial)	890602.1		
Major (>20cm long and into subcutaneous tissue)	890604.2		
Avulsion NFS	890800.1		
Superficial (<100cm^2)	890802.1		
Major (>100cm^2)	890804.2		

Muscle-Tendons-Ligaments:

Injured Area	**AIS Code**	**Right**	**Left**
Collateral or Cruciate Ligament Laceration (rupture, tear, avulsion)	840404.2		
MCL and ACL tear???			
Muscle Laceration (rupture, tear, avulsion)	840600.2		
Muscle Strain or Contusion	840602.1		

Tendon Laceration (rupture, tear, avulsion)	840802.2		
Multiple Tendons	840804.2		
Patellar Tendon Laceration (rupture, tear, avulsion)	841002.2		
Total Transection	841004.2		
Meniscus	N/A		

Skeletal-Joints:

Injured Area	AIS Code	Right	Left
Knee (NFS)	850899.1		
Contusion (includes articular cartilage)	850802.1		
Dislocation (NFS)	850614.2		
Without involving articular cartilage	850614.2		
Involving articular cartilage	850618.2		
Laceration into joint	850622.2		
Meniscus tear	850822.2		
Sprain	850826.2		

Injured Area	AIS Code	Right	Left
Femur fracture NFS	851800.3		
Open/displaced/comminuted	851801.3		
Condylar	851804.3		
Shaft	851804.3		
Supracondylar	851822.3		

Injured Area	AIS Code	Right	Left
Patella fracture	852400.2		

Injured Area	AIS Code	Right	Left
Tibia NFS	853499.1		
Contusion	853402.1		
Fracture any type	853404.2		
Open/displaced/comminuted	853405.3		
Condyles (plateau)	853406.2		
Open/displaced/comminuted	853408.3		
Intercondyloid spine	853410.2		
Shaft	853420.2		
Open/displaced/comminuted	853422.3		

Injured Area	AIS Code	Right	Left
Fibula NFS	851699.1		
Contusion	851602.1		
Fracture any type	851605.2		
Head, neck, shaft	851606.2		

Summary of Autopsy Results:

Right	Left

Assessment of Injury:

	Right	Left
Ligament Displacement (mm)		
Ligament Strain (%)		
Ligament Strain Rate (%/sec)		
Tibial Subluxation (mm)		
Corresponding AIS Injury (Estimation)	See Autopsy Report	

C. Sample Test Checklist

Lateral Tibia Impact Test Procedure Checklist

TEST #: _____ DATE: _____

Notification Phase:

1. ___Mark Whitmer contacts Dr. Bolte and reports that cadaver/lower extremity(s) is/are available.
2. ___Enact cadaver selection algorithm-determine if cadaver is suitable for test (may not be 100% effective in all cases.)
3. ___Determine Preparation and Test Schedule.
4. ___Contact Team Members ( ) and alert to testing course of action.
5. ___Schedule cadaver pickup with gurney from Mark Whitmer in morgue.
6. ___Obtain biohazard bags and boxes from loading dock in Graves Hall, determine and note if cadaver is save/no-save ashes.
7. ___Turn on power to cooler such that it is sufficiently chilled in time to receive lower extremity(s).
8. ___Check charging of batteries in lab, change out of drill/driver if necessary.
9. ___Gather all supplies and equipment from OSU and VRTC **including faro arm**
10. ___Meet at Room 3024 Graves Hall at assigned times.

Cadaver Preparation:
(See Cadaver Selection & Preparation Protocol)
(Events occur in the Morgue)

(**R/L)**

1. ___/__ Ensure that universal precautions are being enforced at all times (proper personal protective equipment, blood-borne pathogen procedures and proper lab techniques used.)
2. ___/__ Wash lower extremity(s) with antiseptic soap and 10% bleach solution.
3. ___/__ Exercise lower extremity(s) through normal range of motion to remove rigor mortis.
4. ___/__ Examine subject lower extremity(s) for anomalies, bruises, abrasions, cuts and scars.
5. ___/__ Label each foot with a “R” or “L” to signify right or left leg respectively.
6. ___/__ Record lower extremity(s) anthropometric measurements (see Anthropometry Protocol.)
7. ___/__ Remove lower extremity(s) from subject at pelvis, making sure to remove femur in one section.
8. ___/__ Record subject information (cadaver number, height, weight, cause of death, age, and gender on data sheet.)

Cadaver Instrumentation:
(See Instrumentation Protocol)

(Left Leg)

1. ___Perform manual drawer tests (A-P) and medial-lateral laxity tests; record results.
2. ___On gurney/table, cut femur, leaving approximately 11" inches from patella.
3. ___Smooth anterior accel location, glue accel block and secure with wire tie, allow to dry over night
4. ___Remove muscle and fascia from proximal 7 cm of femur in preparation for potting.
5. ___Clean and dry femur bone(s) for proper bonding.
6. ___Weigh the lower extremity(s) without shoe (See Pre-Test Data Protocol.)
7. ___Record ACL and MCL length.
8. ___Prepare DVRT with barbs at determined distance from each other.
9. ___Check continuity of system, mark non-sensing end of core and cut core to proper length.
10. ___Prepare digital cameras and initiate still photos during insertion of DVRT's for documentation.
11. ___Attach one DVRT to the ACL. Place sensor end as deep in posterior knee as possible, in line with ACL fibers and connect with core. Make sure wire has some relief so as not to damage leads during testing. **Suture barbs to ACL**
12. ___Attach one DVRT to the MCL. Make sure wire has some relief so as not to damage leads during testing. **Suture barbs to MCL**
13. ___Note which serial number corresponds to which DVRT
14. ___Note barb-barb inserted distance in ACL and MCL.
15. ___Perform anterior and posterior drawer tests to ensure free movement of DVRT core, re-insert DVRT if necessary.
16. ___ Suture exposed flesh and cover to prevent leaking during potting.
17. ___Clean lower extremity with antiseptic solution to remove blood.
18. ___Bring lower extremity into place near fixture.
19. ___Mix body filler with hardener.
20. ___Pot exposed femur in steel cup with body filler securing in place. **Make certain thigh and leg are vertical and in line with rotation pin.**
    a. Use set screws to initially hold femur in-line.
    b. Fill with BONDO and allow to set.
21. ___Wait 30 minutes for body filler to harden completely.
22. ___Attach Femoral tri-axial accelerometer
23. ___Attach anterior tibial tri-axial accelerometer.
24. ___Ensure all accelerometer wires have some relief so as not to damage leads during testing.
25. ___Attach photo-target stickers to tibia.
26. ___Take all required positional and anthropometric measurements (Pre-Test Positioning Measurements sheet).
27. ___Raise leg into position with string- Take FARO pts in new position
28. ___Check previous section and all measurement sheets for completion of all steps.
29. ___Make sure all faro arm measurements are saved

Test Performance Phase and Positioning:
(See Positioning & Instrumentation Measurements Protocol)

(Left leg)

1. _/_/_/_/_Ensure that universal precautions are being enforced.
2. _/_/_/_/_Make sign board.
3. _/_/_/_/_Configure Yokogawa data acquisition system (See Yokogawa Operating Instructions.)
4. _/_/_/_/_Set-up high speed camera and lighting and flash.
5. _/_/_/_/_Check connection of tibial and femoral accelerometers, and light traps.
6. _/_/_/_/_Record the distance from the cameras to the tibial photo target.
7. _/_/_/_/_Connect all instrumentation, verify continuity, balance, etc.
8. _/_/_/_/_Position event tape load cell and lower extremity; hook up event switches.
9. _/_/_/_/_Zero all recording channels.
10. _/_/_/_/_Zero light trap reading.
11. _/_/_/_/_Double check photographic targets.
12. _/_/_/_/_Place inch tape in field of view for photographic analysis.
13. _/_/_/_/_Place sign board.
14. _/_/_/_/_ Position leg at corresponding height from bottom dead center and Faro Accels (See Test Matrix) (Height is measured from mark 21" down from rotation point on tibia)
15. _/_/_/_/_Still photography.
16. _/_/_/_/_Final camera focus.
17. _/_/_/_/_Ensure all test data sheets are complete (See Test Data Protocol.)
18. _/_/_/_/_**TURN FLASH ON.**
19. _/_/_/_/_Check previous page for completion of all steps.
20. _/_/_/_/_Conduct test.
21. _/_/_/_/_Check knee, data and video for injury before next test

Cadaver Instrumentation:
(See Instrumentation Protocol)

(**Right Leg**)

1. ___Perform manual drawer tests (A-P) and medial-lateral laxity tests; record results.
2. ___On gurney/table, cut femur, leaving approximately 11" inches from patella.
3. ___Smooth anterior accel location, glue accel block and secure with wire tie, allow to dry over night
4. ___Remove muscle and fascia from proximal 7 cm of femur in preparation for potting.
5. ___Clean and dry femur bone(s) for proper bonding.
6. ___Weigh the lower extremity(s) without shoe (See Pre-Test Data Protocol.)
7. ___Record ACL and MCL length.
8. ___Prepare DVRT with barbs at determined distance from each other.
9. ___Check continuity of system, mark non-sensing end of core and cut core to proper length.

10. ___Prepare digital cameras and initiate still photos during insertion of DVRT's for documentation.
11. ___Attach one DVRT to the ACL. Place sensor end as deep in posterior knee as possible, in line with ACL fibers and connect with core. Make sure wire has some relief so as not to damage leads during testing. **Suture barbs to ACL**
12. ___Attach one DVRT to the MCL. Make sure wire has some relief so as not to damage leads during testing. **Suture barbs to MCL**
13. ___Note which serial number corresponds to which DVRT
14. ___Note barb-barb inserted distance in ACL and MCL.
15. ___Perform anterior and posterior drawer tests to ensure free movement of DVRT core, re-insert DVRT if necessary.
16. ___ Suture exposed flesh and cover to prevent leaking during potting.
17. ___Clean lower extremity with antiseptic solution to remove blood.
18. ___Bring lower extremity into place near fixture.
19. ___Mix body filler with hardener.
20. ___Pot exposed femur in steel cup with body filler securing in place. **Make certain thigh and leg are vertical and in line with rotation pin.**
    a. Use set screws to initially hold femur in-line.
    b. Fill with BONDO and allow to set.
21. ___Wait 30 minutes for body filler to harden completely.
22. ___Attach Femoral tri-axial accelerometer
23. ___Attach anterior tibial tri-axial accelerometer.
24. ___Ensure all accelerometer wires have some relief so as not to damage leads during testing.
25. ___Attach photo-target stickers to tibia.
26. ___Take all required positional and anthropometric measurements (Pre-Test Positioning Measurements sheet).
27. ___Raise leg into position with string- Take FARO pts in new position
28. ___Check previous section and all measurement sheets for completion of all steps.
29. ___Make sure all faro arm measurements are saved

Test Performance Phase and Positioning:
(See Positioning & Instrumentation Measurements Protocol)

(Right leg)

1. _/_/_/_/_Ensure that universal precautions are being enforced.
2. _/_/_/_/_Make sign board.
3. _/_/_/_/_Configure Yokogawa data acquisition system (See Yokogawa Operating Instructions.)
4. _/_/_/_/_Set-up high speed camera and lighting and flash.
5. _/_/_/_/_Check connection of tibial and femoral accelerometers, and light traps.
6. _/_/_/_/_Record the distance from the cameras to the tibial photo target.
7. _/_/_/_/_Connect all instrumentation, verify continuity, balance, etc.

8. _/_/_/_/_Position event tape load cell and lower extremity; hook up event switches.
9. _/_/_/_/_Zero all recording channels.
10. _/_/_/_/_Zero light trap reading.
11. _/_/_/_/_Double check photographic targets.
12. _/_/_/_/_Place inch tape in field of view for photographic analysis.
13. _/_/_/_/_Place sign board.
14. _/_/_/_/_ Position leg at corresponding height from bottom dead center and Faro Accels (See Test Matrix) (Height is measured from mark 21" down from rotation point on tibia)
15. _/_/_/_/_Still photography.
16. _/_/_/_/_Final camera focus.
17. _/_/_/_/_Ensure all test data sheets are complete (See Test Data Protocol.)
18. _/_/_/_/_**TURN FLASH ON.**
19. _/_/_/_/_Check previous page for completion of all steps.
20. _/_/_/_/_Conduct test.
21. _/_/_/_/_Check knee, data and video for injury before next test

Post-Test:

(**R/L)**

1. ___/__ Ensure that universal precautions are being enforced.
2. ___/__ Record velocity from light traps, pressure, date, time, etc.
3. ___/__ Still photography.
4. ___/__ Download the data from the high-speed cameras.
5. ___/__ Remove lower extremity from the lift table and place on gurney.
6. ___/__ Remove all instrumentation, saving all instruments and noting any irregularities.
7. ___/__ Photograph, record and note any relevant observations.
8. ___/__ Prepare lower extremity for post-MRI and x-ray.

Autopsy/Dissection:

(See Autopsy Dissection Report)

(**R/L)**

1. ___/__ Determine / document trauma; specifically, that involving any ACL or MCL tears and/or avulsion or bone fractures (Refer to.Doc).
2. ___/__ Photograph significant injury.

Laboratory Clean-up:

1. _____ Ensure that universal precautions are being enforced.
2. _____ Complete all steps on the workroom decontamination checklist.
3. _____ Place all contaminated disposables in bio-hazard container.
4. _____ Soak and/or scrub all non-sharp instruments with bleach solution.
5. _____ Scrub counter tops, table tops, impactor surface and gurney with bleach solution.

6. _____ Check instrumentation and cables for any blood contamination, and if found, remove with bleach solution.
7. _____ Sweep and mop floor with bleach solution.
8. _____ Complete all steps on the hand washing station inspection checklist.
9. _____ Check stock of protective clothing and, if necessary, restock for next test.
10. _____ Check previous section for completion of all steps.
11. _____ Sign and date the workroom decontamination checklist.
12. _____ Return all specimen remains to Mark Whitmer in OSU morgue.
13. _____ Prepare Biohazard box for collection and call Environmental Health and Safety for Biohazard Pickup (Tuesdays and Thursdays.)

Miscellaneous Test Notes:

D. Sample Decontamination Checklist

DECONTAMINATION CHECKLIST
Room 3024 Graves Hall

Initials **Task**

_____ _____ gallons of disinfectant solution (2 oz. Chlorine bleach and 1 gallon fresh water) were prepared at Time:_____ on Date:_____ (**MUST BE PREPARED FRESH FOR EACH TEST!**) by:_____.

_____All areas with gross contamination by blood or other potentially infectious materials were wiped clean using appropriately absorbent materials.

_____The operating table, gurney and all countertops, bench-tops and other surfaces which may have been contaminated by blood or other potentially infectious materials were flooded with disinfectant solution and wiped dry with clean, absorbent, disposable towels.

_____All contaminated goggles, hand tools, re-useable sharps, measuring instruments and mounting blocks were cleaned of gross contamination over the sink, submersed in disinfectant solution and wiped dry with clean, absorbent, disposable towels.

_____Those items that cannot be submersed (e.g. Electronic instruments and hand tools) were thoroughly wiped with a clean, disposable towel soaked in disinfectant solution and wiped dry with clean, absorbent, disposable towels.

_____The impactor face was thoroughly wiped with a clean, disposable towel soaked in disinfectant solution and wiped dry with clean, absorbent disposable towels.

_____All disposable towels, cover-alls, shoe covers, gloves, etc. were collected in the appropriately labeled containers.

_____The floor of the room was mopped with disinfectant solution.

_____The mop was rinsed in fresh disinfectant solution.

_____The floor of the room was mopped with a regular detergent solution.

_____The red liner bags containing contaminated disposables were closed and placed in the holding area.

_____The inside and outer surfaces of the contaminated disposables container were thoroughly wiped with a clean, disposable towel soaked in disinfectant solution and wiped dry with clean, absorbent, disposable towels. And clean red liner bags were installed.

_____The sink was cleared of visible contamination, thoroughly wiped with a clean, disposable towel soaked in disinfectant solution and flushed with fresh water.

_____ _____

Signature Date

HANDWASHING STATION INSPECTION CHECKLIST

Sufficient quantities of non-abrasive soap, waterless cleaning solution or clean, solution impregnated towels are present.

Sufficient quantities of dry, absorbent paper towels are present.

The eyewash kit is present and in good working condition.

A properly labeled container for discarded towels is located nearby.

_____ _____

Signature Date

E. Sample Instrumentation Configuration

Chn	Channel Name	Engineering Units	Cal File Manufacturer/Model/Serial	Excit Volts	Sensitivity mV/V/Unit	Transducer Full Scale	Selected Full Scale
1	Event	V	Event-1-1.cal	10	100	10	10
2	LOADFX	N	Denton-2944-122FX.cal	10	0.0003933	4448	6356.471
3	LOADFY	N	Denton-2944-122FZ.cal	10	0.0001728	6672	14467.59
4	LOADFZ	N	Denton-2944-122FY.cal	10	0.0003931	4448	6359.705
5	LOADMX	NM	Denton-2944-122MX.cal	10	0.0095761	169	261.0666
6	LOADMY	NM	Denton-2944-122MZ.cal	10	0.0160707	113	155.5626
7	LOADMZ	NM	Denton-2944-122MY.cal	10	0.0095208	169	262.583
8	FEMFX	N	Denton-2667-76FX.cal	10	0.000138047	13344	18109.77
9	FEMFY	N	Denton-2667-76FY.cal	10	0.000138737	13344	18019.77
10	FEMFZ	N	Denton-2667-76FZ.cal	10	5.54E-05	13344	18037.31
11	Spare	G	Endevco-7264C-2K TZ-P51299.cal	10	0.02018	2000	2477.701
12	FEMMY	Nm	Denton-2667-76MY.cal	10	0.005000885	339	499.9115
13	FEMMZ	Nm	Denton-2667-76MZ.cal	10	0.009708555	339	515.0097
14	ACLSTRAIN	mm	MicroStrain-M-DVRT-9-1121-0001.cal	1	757	10	13.21004
15	MCLSTRAIN	mm	MicroStrain-M-DVRT-9-1121-0006.cal	1	803	10	12.4533
16	FEMXG	G	Endevco-7264C-2K TZ-P51940.cal	10	0.01929	2000	518.4033
17	FEMYG	G	Endevco-7264C-2K TZ-P51935.cal	10	0.02056	2000	486.3813
18	FEMZG	G	Endevco-7264C-2K TZ-P51328.cal	10	0.01868	2000	535.3319
19	FEMWX	deg/sec	DTS-ARS-1500-ARS1039.cal	5	0.253	1000	1581.028
20	FEMWY	deg/sec	DTS-ARS-1500-ARS1101.cal	5	0.2482	1000	1611.604
21	FEMWZ	deg/sec	DTS-ARS-1500-ARS1100.cal	5	0.262	1000	1526.718
22	ANTTIBXG	g	Entran-EGEB6Q-06A04R09.cal	10	0.02288	2000	437.0629
23	ANTTIBYG	G	Entran-EGEBQ-99I02F06.cal	10	0.01868	2000	535.3319
24	ANTTIBZG	G	Entran-EGEB6Q-06A04R05.cal	10	0.02351	2000	425.3509
25	ANTTIBWX	deg/sec	DTS-ARS-12K-ARS1087.cal	5	0.02756	1500	3628.447
26	ANTTIBWY	deg/sec	DTS-ARS-12K-ARS0247.cal	5	0.02838	1500	3523.608
27	ANTTIBWZ	deg/sec	DTS-ARS-12K-ARS1082.cal	5	0.02702	1500	3700.962
28	FEMMX	Nm	Denton-2667-76MX.cal	10	0.004993215	339	500.6794

F. Faro Arm Checklist

Faro Arm measurements		
File name of Faro arm measurements		
Units of Faro arm measurement		
	Right	**Left**
	(Point number)	**(Point number)**
Pre-Test Anthropometric Measurements		
(taken after leg is in position and potted)		
Most Inferior posterior point of calcaneus		
Insertion of patellar tendon on tibial tuberosity		
Proximal medial margin of malleolus		
superior head of fibula		
medial tibial condyle		
medial femoral condyle		
lateral femoral condyle		
anterior tibia superior		
anterior tibia (Measured Point 21" from rotation pt.)		
anterior tibia inferior		
Pre Test Positioning Measurements	**Right**	**Left**
Impact location (Bottom of Plate)		
Femoral tri-axial accel **(In a clockwise fashion looking at the block dimples** **See figure below)**		
1. Dimple 1 (Accel 1 – FEMG1 /)		
2. Dimple 2 (Accel 2 – FEMG2 /)		
3. Dimple 3 (Accel 3 – FEMG3 /)		

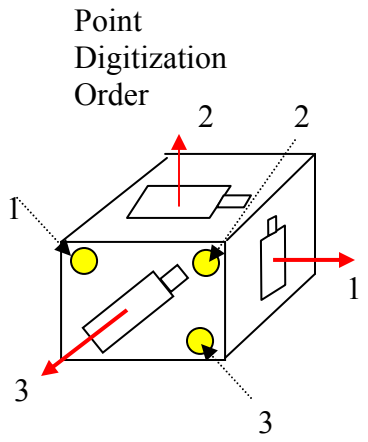

Tibial tri-axial accel (In a clockwise fashion looking at the block dimples) See figure above		
	Right	**Left**
1. Dimple 1 (Accel 1 – ANTIBG1 /)		
2. Dimple 2 (Accel 2 – ANTIBG2 /)		
3. Dimple 3 (Accel 3 – ANTIBG3 /)		
*** accelerometer reads (-) according to J211, R denotes right leg only**		
Femoral Load Cell(all four corners)		
1. Anterior		
2. Lateral		
3. Posterior		
4. Medial		

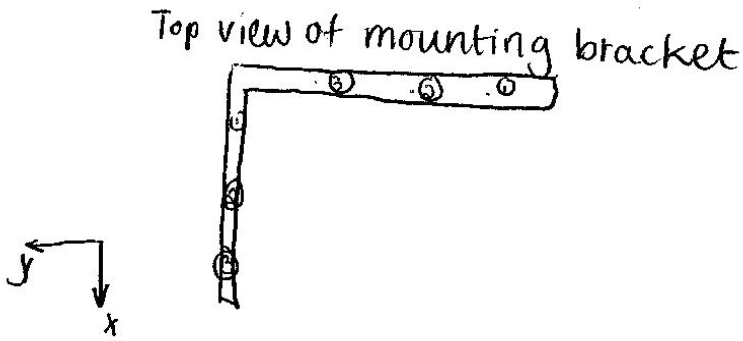

Mounting Bracket to Establish Coordinate System		
See figure above		
	Right	Left
1. Dimple 1 (Mounting Block Y-Direction)		
2. Dimple 2 (Mounting Block Y-Direction)		
3. Dimple 3 (Mounting Block Y-Direction)		
1. Dimple 1 (Mounting Block X-Direction)		
2. Dimple 2 (Mounting Block X-Direction)		
3. Dimple 3 (Mounting Block X-Direction)		
Fiducials- Superior to Inferior	Right	Left
Bracket		
Femur Cup		
Femur Superior		
Femur Inferior		
Knee		
Tibia Superior		
Tibia Inferior		

Leg Raise to Starting Position

Trial Name: (_____)

Pre Test Positioning Measurements	**Right**	**Left**
Femoral tri-axial accel (In a clockwise fashion looking at the block dimples See figure below)		
1. Dimple 1 (Accel 1 – FEMG1 /)		
2. Dimple 2 (Accel 2 – FEMG2 /)		
3. Dimple 3 (Accel 3 – FEMG3 /)		

Point Digitization Order

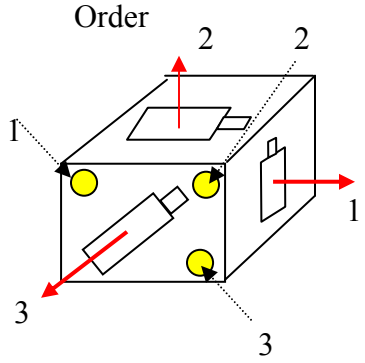

Tibial tri-axial accel (In a clockwise fashion looking at the block dimples) See figure above		
	Right	**Left**
1. Dimple 1 (Accel 1 – ANTIBG1 /)		
2. Dimple 2 (Accel 2 – ANTIBG2 /)		
3. Dimple 3 (Accel 3 – ANTIBG3 /)		

G. MATLAB Code

```
      clc
close all
acl=38; % ACL Length %mm
aclbl=17; %ACL Barb Distance %mm
mcl=55; % MCL Length %mm
mclbl=17; %MCL Barb Distance %mm
%% 0901PED04R01
R01 = csvread('0901PED04R01.csv',16,0);
time01=R01(:,1);
ACLSTRAINR01=R01(:,15);
ACLSTRETCHR01=-ACLSTRAINR01.*acl./aclbl;
Max_ACLSTRETCHR01=max(ACLSTRETCHR01)
MCLSTRAINR01=R01(:,16);
MCLSTRETCHR01=-MCLSTRAINR01.*mcl./mclbl;
Max_MCLSTRETCH01=max(MCLSTRETCHR01)
ImpactForceY01=-R01(:,4);
Max_ImpactForceY01=max(ImpactForceY01)
FemurForceY01=-R01(:,10);
Max_FemurForceY01=max(FemurForceY01)
%% 0901PED07R02
%% 0901PED07R03
R03 = csvread('0901PED07R03.csv',16,0);
time03=R03(:,1);
ACLSTRAINR03=R03(:,15);
ACLSTRETCHR03=-ACLSTRAINR03.*acl./aclbl;
Max_ACLSTRETCHR03=max(ACLSTRETCHR03)
MCLSTRAINR03=R03(:,16);
MCLSTRETCHR03=-MCLSTRAINR03.*mcl./mclbl;
Max_MCLSTRETCH03=max(MCLSTRETCHR03)
ImpactForceY03=-R03(:,4);
Max_ImpactForceY03=max(ImpactForceY03)
FemurForceY03=-R03(:,10);
Max_FemurForceY03=max(FemurForceY03)
%% 0901PED04R04
R04 = csvread('0901PED04R04.csv',16,0);
time04=R04(:,1);
ACLSTRAINR04=R04(:,15);
ACLSTRETCHR04=-ACLSTRAINR04.*acl./aclbl;
Max_ACLSTRETCHR04=max(ACLSTRETCHR04)
MCLSTRAINR04=R04(:,16);
MCLSTRETCHR04=-MCLSTRAINR04.*mcl./mclbl;
Max_MCLSTRETCH04=max(MCLSTRETCHR04)
ImpactForceY04=-R04(:,4);
Max_ImpactForceY04=max(ImpactForceY04)
FemurForceY04=-R04(:,10);
Max_FemurForceY04=max(FemurForceY04)
%% 0901PED10R05
R05 = csvread('0901PED10R05.csv',16,0);
time05=R05(:,1);
ACLSTRAINR05=R05(:,15);
ACLSTRETCHR05=-ACLSTRAINR05.*acl./aclbl;
Max_ACLSTRETCHR05=max(ACLSTRETCHR05)
MCLSTRAINR05=R05(:,16);
MCLSTRETCHR05=-MCLSTRAINR05.*mcl./mclbl;
Max_MCLSTRETCH05=max(MCLSTRETCHR05)
ImpactForceY05=-R05(:,4);
Max_ImpactForceY05=max(ImpactForceY05)
FemurForceY05=-R05(:,10);
Max_FemurForceY05=max(FemurForceY05)
%% 0901PED04R06
R06 = csvread('0901PED04R06.csv',16,0);
time06=R06(:,1);
```

```
ACLSTRAINR06=R06(:,15);
ACLSTRETCHR06=-ACLSTRAINR06.*acl./aclbl;
Max_ACLSTRETCHR06=max(ACLSTRETCHR06)
MCLSTRAINR06=R06(:,16);
MCLSTRETCHR06=-MCLSTRAINR06.*mcl./mclbl;
Max_MCLSTRETCH06=max(MCLSTRETCHR06)
ImpactForceY06=-R06(:,4);
Max_ImpactForceY06=max(ImpactForceY06)
FemurForceY06=-R06(:,10);
Max_FemurForceY06=max(FemurForceY06)
%% 0901PED14R07
R07 = csvread('0901PED14R07.csv',16,0);
time07=R07(:,1);
ACLSTRAINR07=R07(:,15);
ACLSTRETCHR07=-ACLSTRAINR07.*acl./aclbl;
Max_ACLSTRETCHR07=max(ACLSTRETCHR07)
MCLSTRAINR07=R07(:,16);
MCLSTRETCHR07=-MCLSTRAINR07.*mcl./mclbl;
Max_MCLSTRETCH07=max(MCLSTRETCHR07)
ImpactForceY07=-R07(:,4);
Max_ImpactForceY07=max(ImpactForceY07)
FemurForceY07=-R07(:,10);
Max_FemurForceY07=max(FemurForceY07)
%% 0901PED04R08
R08 = csvread('0901PED04R08.csv',16,0);
time08=R08(:,1);
ACLSTRAINR08=R08(:,15);
ACLSTRETCHR08=-ACLSTRAINR08.*acl./aclbl;
Max_ACLSTRETCHR08=max(ACLSTRETCHR08)
MCLSTRAINR08=R08(:,16);
MCLSTRETCHR08=-MCLSTRAINR08.*mcl./mclbl;
Max_MCLSTRETCH08=max(MCLSTRETCHR08)
ImpactForceY08=-R08(:,4);
Max_ImpactForceY08=max(ImpactForceY08)
FemurForceY08=-R08(:,10);
Max_FemurForceY08=max(FemurForceY08)
%% 0901PED19R09
R09 = csvread('0901PED19R09.csv',16,0);
time09=R09(:,1);
ACLSTRAINR09=R09(:,15);
ACLSTRETCHR09=-ACLSTRAINR09.*acl./aclbl;
Max_ACLSTRETCHR09=max(ACLSTRETCHR09)
MCLSTRAINR09=R09(:,16);
MCLSTRETCHR09=-MCLSTRAINR09.*mcl./mclbl;
Max_MCLSTRETCH09=max(MCLSTRETCHR09)
ImpactForceY09=-R09(:,4);
Max_ImpactForceY09=max(ImpactForceY09)
FemurForceY09=-R09(:,10);
Max_FemurForceY09=max(FemurForceY09)
%% 0901PED04R10
R10 = csvread('0901PED04R10.csv',16,0);
time10=R10(:,1);
ACLSTRAINR10=R10(:,15);
ACLSTRETCHR10=-ACLSTRAINR10.*acl./aclbl;
Max_ACLSTRETCHR10=max(ACLSTRETCHR10)
MCLSTRAINR10=R10(:,16);
MCLSTRETCHR10=-MCLSTRAINR10.*mcl./mclbl;
Max_MCLSTRETCH10=max(MCLSTRETCHR10)
ImpactForceY10=-R10(:,4);
Max_ImpactForceY10=max(ImpactForceY10)
FemurForceY10=-R10(:,10);
Max_FemurForceY10=max(FemurForceY10)
%% 0901PED19WR11
R11 = csvread('0901PED19WR11.csv',16,0);
```

```
time11=R11(:,1);
ACLSTRAINR11=R11(:,15);
ACLSTRETCHR11=-ACLSTRAINR11.*acl./aclbl;
Max_ACLSTRETCHR11=max(ACLSTRETCHR11)
MCLSTRAINR11=R11(:,16);
MCLSTRETCHR11=-MCLSTRAINR11.*mcl./mclbl;
Max_MCLSTRETCH11=max(MCLSTRETCHR11)
ImpactForceY11=-R11(:,4);
Max_ImpactForceY11=max(ImpactForceY11)
FemurForceY11=-R11(:,10);
Max_FemurForceY11=max(FemurForceY11)
%% 0901PED04R12
R12 = csvread('0901PED04R12.csv',16,0);
time12=R12(:,1);
ACLSTRAINR12=R12(:,15);
ACLSTRETCHR12=-ACLSTRAINR12.*acl./aclbl;
Max_ACLSTRETCHR12=max(ACLSTRETCHR12)
MCLSTRAINR12=R12(:,16);
MCLSTRETCHR12=-MCLSTRAINR12.*mcl./mclbl;
Max_MCLSTRETCH12=max(MCLSTRETCHR12)
ImpactForceY12=-R12(:,4);
Max_ImpactForceY12=max(ImpactForceY12)
FemurForceY12=-R12(:,10);
Max_FemurForceY12=max(FemurForceY12)
%% Comparison Plots
%% ACL Stretch
figure
plot(time01,ACLSTRETCHR01,':','LineWidth',2)
hold on
plot(time03,ACLSTRETCHR03,'g','LineWidth',2)
plot(time04,ACLSTRETCHR04,':g','LineWidth',2)
plot(time05,ACLSTRETCHR05,'r','LineWidth',2)
plot(time06,ACLSTRETCHR06,':r','LineWidth',2)
plot(time07,ACLSTRETCHR07,'c','LineWidth',2)
plot(time08,ACLSTRETCHR08,':c','LineWidth',2)
plot(time09,ACLSTRETCHR09,'m','LineWidth',2)
plot(time10,ACLSTRETCHR10,':m','LineWidth',2)
plot(time11,ACLSTRETCHR11,'k','LineWidth',2)
plot(time12,ACLSTRETCHR12,':k','LineWidth',2)
hold off
title('Comparison ACL Stretch with Different Loading')
xlabel('Time (s)')
ylabel('Stretch (mm)')
legend('0901PED04R01','0901PED07R03','0901PED04R04','0901PED10R05','0901PED04R
06','0901PED14R07','0901PED04R08','0901PED19R09','0901PED04R10','0901PED19WR11
','0901PED04R12"')
axis([-.2 .5 -.5 4.5])
grid on
%% MCL Stretch
figure
plot(time01,MCLSTRETCHR01,':','LineWidth',2)
hold on
plot(time03,MCLSTRETCHR03,'g','LineWidth',2)
plot(time04,MCLSTRETCHR04,':g','LineWidth',2)
plot(time05,MCLSTRETCHR05,'r','LineWidth',2)
plot(time06,MCLSTRETCHR06,':r','LineWidth',2)
plot(time07,MCLSTRETCHR07,'c','LineWidth',2)
plot(time08,MCLSTRETCHR08,':c','LineWidth',2)
plot(time09,MCLSTRETCHR09,'m','LineWidth',2)
plot(time10,MCLSTRETCHR10,':m','LineWidth',2)
plot(time11,MCLSTRETCHR11,'k','LineWidth',2)
plot(time12,MCLSTRETCHR12,':k','LineWidth',2)
title('Comparison MCL Stretch with Different Loading')
xlabel('Time (s)')
```

```
ylabel('Stretch (mm)')
legend('0901PED04R01','0901PED07R03','0901PED04R04','0901PED10R05','0901PED04R
06','0901PED14R07','0901PED04R08','0901PED19R09','0901PED04R10','0901PED19WR11
','0901PED04R12"')
axis([-.2 1.2 -3 6])
grid on
%% Impact Force
figure
plot(time01,ImpactForceY01,':','LineWidth',2)
hold on
plot(time03,ImpactForceY03,'g','LineWidth',2)
plot(time04,ImpactForceY04,':g','LineWidth',2)
plot(time05,ImpactForceY05,'r','LineWidth',2)
plot(time06,ImpactForceY06,':r','LineWidth',2)
plot(time07,ImpactForceY07,'c','LineWidth',2)
plot(time08,ImpactForceY08,':c','LineWidth',2)
plot(time09,ImpactForceY09,'m','LineWidth',2)
plot(time10,ImpactForceY10,':m','LineWidth',2)
plot(time11,ImpactForceY11,'k','LineWidth',2)
plot(time12,ImpactForceY12,':k','LineWidth',2)
hold off
title('Comparison Impact Force with Different Loading')
xlabel('Time (s)')
ylabel('Force (N)')
legend('0901PED04R01','0901PED07R03','0901PED04R04','0901PED10R05','0901PED04R
06','0901PED14R07','0901PED04R08','0901PED19R09','0901PED04R10','0901PED19WR11
','0901PED04R12"')
%axis([-.2 1.2 -3 6])
grid on
%% Femur Force
figure
plot(time01,FemurForceY01,':','LineWidth',2)
hold on
plot(time03,FemurForceY03,'g','LineWidth',2)
plot(time04,FemurForceY04,':g','LineWidth',2)
plot(time05,FemurForceY05,'r','LineWidth',2)
plot(time06,FemurForceY06,':r','LineWidth',2)
plot(time07,FemurForceY07,'c','LineWidth',2)
plot(time08,FemurForceY08,':c','LineWidth',2)
plot(time09,FemurForceY09,'m','LineWidth',2)
plot(time10,FemurForceY10,':m','LineWidth',2)
plot(time11,FemurForceY11,'k','LineWidth',2)
plot(time12,FemurForceY12,':k','LineWidth',2)
hold off
title('Comparison Femur Force with Different Loading')
xlabel('Time (s)')
ylabel('Force (N)')
legend('0901PED04R01','0901PED07R03','0901PED04R04','0901PED10R05','0901PED04R
06','0901PED14R07','0901PED04R08','0901PED19R09','0901PED04R10','0901PED19WR11
','0901PED04R12')
%axis([-.2 1.2 -3 6])
grid on

%% Matt Kremer
% 0901PED Angle Analysis
clear all
close all
clc

%% Load Files
R01=csvread('04R01.csv',10,0);
R02=csvread('07R02.csv',10,0);
R03=csvread('07R03.csv',10,0);
R04=csvread('04R04.csv',10,0);
```

```
R05=csvread('10R05.csv',10,0);
R06=csvread('04R06.csv',10,0);
R07=csvread('14R07.csv',10,0);
R08=csvread('04R08.csv',10,0);
R09=csvread('19R09.csv',10,0);
R10=csvread('04R10.csv',10,0);
R11=csvread('19WR11.csv',10,0);
R12=csvread('04R12.csv',10,0);

%% Time
timeR01=R01(:,1);
timeR02=R02(:,1);
timeR03=R03(:,1);
timeR04=R04(:,1);
timeR05=R05(:,1);
timeR06=R06(:,1);
timeR07=R07(:,1);
timeR08=R08(:,1);
timeR09=R09(:,1);
timeR10=R10(:,1);
timeR11=R11(:,1);
timeR12=R12(:,1);

%% Angle
angle01=R01(:,2)+173.1440;
angle02=R02(:,2)+174.2690;
angle03=R03(:,2)+174.0780;
angle04=R04(:,2)+173.7460;
angle05=R05(:,2)+174.1510;
angle06=R06(:,2)+173.8490;
angle07=R07(:,2)+174.1610;
angle08=R08(:,2)+173.6960;
angle09=R09(:,2)+174.5930;
angle10=R10(:,2)+173.8710;
angle11=R11(:,2)+173.8760;
angle12=R12(:,2)+173.5860;
%% Max Angle
max01=max(angle01)
max02=max(angle02)
max03=max(angle03)
max04=max(angle04)
max05=max(angle05)
max06=max(angle06)
max07=max(angle07)
max08=max(angle08)
max09=max(angle09)
max10=max(angle10)
max11=max(angle11)
max12=max(angle12)
%% Plot
figure
plot(timeR01,angle01,':','LineWidth',2)
hold on
plot(timeR02,angle02,'b','LineWidth',2)
plot(timeR03,angle03,'g','LineWidth',2)
plot(timeR04,angle04,':g','LineWidth',2)
plot(timeR05,angle05,'r','LineWidth',2)
plot(timeR06,angle06,':r','LineWidth',2)
plot(timeR07,angle07,'c','LineWidth',2)
plot(timeR08,angle08,':c','LineWidth',2)
plot(timeR09,angle09,'m','LineWidth',2)
plot(timeR10,angle10,':m','LineWidth',2)
plot(timeR11,angle11,'k','LineWidth',2)
plot(timeR12,angle12,':k','LineWidth',2)
```

```
title('Comparison Angular Tibia Deflection Relative to Femur with Different
Loading')
xlabel('Time (ms)')
ylabel('Angle Deflection (degrees)')
legend('0901PED04R01','0901PED07R02','0901PED07R03','0901PED04R04','0901PED10R
05','0901PED04R06','0901PED14R07','0901PED04R08','0901PED19R09','0901PED04R10'
,'0901PED19WR11','0901PED04R12',4)
grid on


close all
clear all
clc
% ------------------------------------------------------------------------
% Written by Yun-Seok Kang, Injury Biomechanics Research Laboratory
% the Ohio State University
% Adapted by Matt Kremer
Updated : 05/02/2009
% ------------------------------------------------------------------------

% 6aw - 6 accels and 3 DTS processing m-file
% First, look at the definition of the body fixed coordinate system on
% aluminum tetrahedron fixture, note that data from tests have to be
% filtered before being imported at this file.
% Input data format: csv or dat will be available
% Input data order: Face 1 - Ax0,Wx1,Ax1, Face 2 - Az0,Wz2,Az2 and
%                   Face 3 - Ay0,Wy3,Ay3, & Wxdot,Wydot,Wzdot & SLDAx
% IMPORTANCE: before run this program please double-check units and still
% picture of the tetrahedron fixture
% Unit: Acc: g , Angular Vel: deg/sec, Angular Acc: rad/sec^2
% - 0: Vertex, Face 1,2 and 3: each surface (pre-defined before the testing
% determine polarity of accelerometers based on instrumentation installed
% See also the document, "6aw analysis method: Euler angle approach"
% written by Yun-Seok Kang, Kevin Moorhouse, John Bolte IV
% Simulation setting
% Define time parameters according to sampling frequency(SmapFreq)
% You have to edit belows according to your testing setup
% ------------------------------------------------------------------------
% Put testing sampling frequency (Hz)
SampFreq = 20000;
% Put the start/end time of the data
Start_time = -0.07; End_time = 0.380;
% Put the initial velocity x,y,z according to SAE J211
Vx0 = 0.0; Vy0 = 0.0; Vz0 = 0.0;
% Loading processed data (filtered by CFC 1000 according to J211)
% file name should be same
load C31.csv;
% Put same name to above but except .csv (i.e data.csv then THAW = data;)
THAW = C31;
% Load data from the FARO measurement (name should be FARO.csv)
load FARO.csv;
% Put row numbers of 1 2 3 points (b, a, c points)
Pt1 = 13; Pt2 = 12; Pt3 = 11;
% ------------------------------------------------------------------------
% Time step
t_step = 1/SampFreq;
```

```
% pol is alway negative in our tetrahedron fixture
pol = 1*9.81;
Rs = pi/180;

% This sequence depends on tests so it needs to be edited
Ax0 = THAW(:,1)*pol;Wx1 = THAW(:,4)*Rs;
Ay0 = THAW(:,2)*pol;Wy3 = THAW(:,5)*Rs;
Az0 = THAW(:,3)*pol;Wz2 = THAW(:,6)*Rs;
Wx_d= THAW(:,7);   Wy_d= THAW(:,8);  Wz_d= THAW(:,9);

Faro = FARO;
% Make a body fixed coordinate system using 3 points
% 3aw block or accel block
S1P = [Faro(Pt1,1),Faro(Pt1,2),Faro(Pt1,3)];
S2P = [Faro(Pt2,1),Faro(Pt2,2),Faro(Pt2,3)];
S3P = [Faro(Pt3,1),Faro(Pt3,2),Faro(Pt3,3)];

% Define the body fixed coordinate system on the 3aw block
% matrix using Euler angle

fy = S2P - S1P;
ufy = fy/norm(fy);
tp_fz = S2P - S3P;
utp_fz = tp_fz/norm(tp_fz);
fx = cross(ufy,utp_fz);
ufx = fx/norm(fx);
fz = cross(ufx,ufy);
ufz = fz/norm(fz);

Ini_A = [ufx',ufy',ufz'];
Ini_Euler_Tet = Func_Y_Euler(Ini_A);

% local vector s' w.r.t block coordinate between cg and s2 point
S = S2P-S2P;
s = Ini_A'*S'/1000;

% Start Euler Parameter and Euler angle approach
% Define intial conditions
% Initial Euler angles
Ang= [Ini_Euler_Tet(1,1),Ini_Euler_Tet(1,2),Ini_Euler_Tet(1,3)];

% Euler angle of the initial orientation
phi_s1(1,1) = Ang(1); phi_s2(1,1)= Ang(2); phi_s3(1,1) =Ang(3);

% Acceleration at the vertex of the tetrahedron fixture
Acc = [Ax0(1,1);Ay0(1,1);Az0(1,1)];

% Initial position (set zero or can put the initial position
DxG(1,1)=0;DyG(1,1)=0;DzG(1,1)=0;

% Generalized coordinate
Q = [DxG;DyG;DzG;phi_s1;phi_s2;phi_s3];
V = Q(4:6);
U = Q(1:3);
```

```
% Initial acceleration from accels
% Transform translational acceleration(body fixed) to Global
AccG = Func_Y_A(Q)*Acc;
AxG(1,1) = AccG(1,1);
AyG(1,1) = AccG(2,1);
AzG(1,1) = AccG(3,1);

% Initial angular acceleration using 6aw kinematic eqs
Wx_dot(1,1) = Wx_d(1,1);
Wy_dot(1,1) = Wy_d(1,1);
Wz_dot(1,1) = Wz_d(1,1);
Wdot = [Wx_dot(1,1);Wy_dot(1,1);Wz_dot(1,1)];

% Initial angular velocity from DTS ARS
Wx(1,1)=Wx1(1,1); Wy(1,1)=Wy3(1,1); Wz(1,1)=Wz2(1,1);
Wo = [Wx(1,1);Wy(1,1);Wz(1,1)];

% Second derivative of the generalized coordinate
U_ddot = [AxG;AyG;AzG];
V_ddot = [Wx_dot;Wy_dot;Wz_dot];
Q_ddot = [U_ddot;V_ddot];

% Initial velocity
VxG(1,1)=AxG*t_step+Vx0 ;VyG(1,1)=AyG*t_step+Vy0; VzG(1,1)=AzG*t_step+Vz0;

% First derivative of the generalized coordinate
U_dot = [VxG;VyG;VzG];
V_dot = [Wx;Wy;Wz];
Q_dot = [U_dot;V_dot];

% Kinematic Analysis at Head CG
% Position analysis
% s: position vector relative to body fixed coordinate system
% Func_A(Q)* s: transform s to S which is same global position vector

Rp = Q(1:3)+ Func_Y_A(Q)* s;
rpxG(1,1)=Rp(1,1);
rpyG(1,1)=Rp(2,1);
rpzG(1,1)=Rp(3,1);

% Velocity analysis
W_tilda = Func_Tilda(Wo);
s_tilda = Func_Tilda(s);

Rp_dot = Q_dot(1:3)+Func_Y_A(Q)*W_tilda* s;
rpx_dotG(1,1)=Rp_dot(1,1);
rpy_dotG(1,1)=Rp_dot(2,1);
rpz_dotG(1,1)=Rp_dot(3,1);

% Transform angular velocity to Global coordinate
% Determine time derivative of Euler anlge, Phi31_dot, Phi11_dot, Phi32_dot
H = Func_Y_H(Q);
Euler_dot = inv(H)*V_dot;
Phi31_dot(1,1)=Euler_dot(1,1);
```

```
Phi11_dot(1,1)=Euler_dot(2,1);
Phi32_dot(1,1)=Euler_dot(3,1);

% Check the WG using the other equation
WG = Func_Y_A(Q)*W_tilda*Func_Y_A(Q)';
WxG(1,1)= WG(3,2);
WyG(1,1)= WG(1,3);
WzG(1,1)= WG(2,1);

% Global Angular Displacement
AnDxG(1,1)=WxG*t_step ;AnDyG(1,1)=WyG*t_step; AnDzG(1,1)=WzG*t_step;

% Check the Wx, Wy, Wz
A1 = Func_Y_A(Q);
WGg = [WxG(1,1);WyG(1,1);WzG(1,1)];
RWG_tilda = Func_Tilda(WGg);
B1 = A1'*RWG_tilda*A1;
TWx(1,1) = B1(3,2);
TWy(1,1) = B1(1,3);
TWz(1,1) = B1(2,1);

% Acceleration analysis
W_dot_tilda = Func_Tilda(Wdot);
Rp_ddot = Q_ddot(1:3)+(Func_Y_A(Q)*W_dot_tilda+Func_Y_A(Q)*W_tilda*W_tilda)*
s;
rpx_ddotG(1,1)=Rp_ddot(1,1);
rpy_ddotG(1,1)=Rp_ddot(2,1);
rpz_ddotG(1,1)=Rp_ddot(3,1);

% Acceleration analysis (the other way)
NRp_ddot = Q_ddot(1:3)-
Func_Y_A(Q)*s_tilda*[Wx_dot(1,1);Wy_dot(1,1);Wz_dot(1,1)]-
Func_Y_A(Q)*W_tilda*s_tilda* [Wx(1,1);Wy(1,1);Wz(1,1)];
Nrpx_ddotG(1,1)=NRp_ddot(1,1);
Nrpy_ddotG(1,1)=NRp_ddot(2,1);
Nrpz_ddotG(1,1)=NRp_ddot(3,1);

% Transform Angular acceleration to Global coordinate
W_dotG = Func_Y_A(Q)*W_dot_tilda*Func_Y_A(Q)';
Wx_dotG(1,1) = W_dotG(3,2);
Wy_dotG(1,1) = W_dotG(1,3);
Wz_dotG(1,1) = W_dotG(2,1);

% Update generalized coordinate
V = V + Euler_dot*t_step;
U = U + U_dot*t_step;
Q = [U;V];

Time(1,1)=Start_time;
i =1;

% Time loop to run kinematic analysis
for t = Start_time+t_step:t_step:End_time

    % At the vertex of the fixture
```

```
    % ACCELERATION
    % Transform translational acceleration to global coordinate system
    AccG = Func_Y_A(Q)*[Ax0(i+1,1);Ay0(i+1,1);Az0(i+1,1)];
    AxG(i+1,1) = AccG(1,1);
    AyG(i+1,1) = AccG(2,1);
    AzG(i+1,1) = AccG(3,1);

    % Angular acceleration from 6aw Equation (See 6aw analysis method- Euler
angle approach)
    Wx_dot(i+1,1) = Wx_d(i+1,1);
    Wy_dot(i+1,1) = Wy_d(i+1,1);
    Wz_dot(i+1,1) = Wz_d(i+1,1);

    % Updating 2nd derivative of generalized coordinate
    U_ddot = [AxG(i+1,1);AyG(i+1,1);AzG(i+1,1)];
    V_ddot = [Wx_dot(i+1,1);Wy_dot(i+1,1);Wz_dot(i+1,1)];
    Q_ddot = [U_ddot;V_ddot];

    Wo = [Wx1(i+1,1);Wy3(i+1,1);Wz2(i+1,1)];

    % VELOCITY
    % Angular velocity from DTS angular rate sensor
    % Wx1; Wy3 ;Wz2 w.r.t body fixed coordinate
    Wx(i+1,1)=Wx1(i+1,1); Wy(i+1,1)=Wy3(i+1,1); Wz(i+1,1)=Wz2(i+1,1);

    % Calculate translational velocity(global coordinate) by integrating
accelerations
    VxG(i+1,1)=VxG(i,1)+ 0.5*(AxG(i,1)+AxG(i+1,1))*t_step;
    VyG(i+1,1)=VyG(i,1)+ 0.5*(AyG(i,1)+AyG(i+1,1))*t_step;
    VzG(i+1,1)=VzG(i,1)+ 0.5*(AzG(i,1)+AzG(i+1,1))*t_step;

    % Updating 1st derivative of generalized coordinate
    U_dot = [VxG(i+1,1);VyG(i+1,1);VzG(i+1,1)];
    V_dot = [Wx(i+1,1);Wy(i+1,1);Wz(i+1,1)];
    Q_dot = [U_dot;V_dot];

    % KINEMATICS at Head CG
    % POSITION Analysis

    Rp = Q(1:3)+ Func_Y_A(Q)* s;
    rpxG(i+1,1)=Rp(1,1);
    rpyG(i+1,1)=Rp(2,1);
    rpzG(i+1,1)=Rp(3,1);

    % Velocity analysis
    % Define W_tilda
    W_tilda = Func_Tilda(Wo);
    % Equation for velocity analysis at head cg
    Rp_dot = Q_dot(1:3)+Func_Y_A(Q)*W_tilda* s;
    rpx_dotG(i+1,1)=Rp_dot(1,1);
    rpy_dotG(i+1,1)=Rp_dot(2,1);
    rpz_dotG(i+1,1)=Rp_dot(3,1);

    % Acceleration analysis
    % Define W_dot_tilda
```

```
    Wdot = [Wx_dot(i+1,1);Wy_dot(i+1,1);Wz_dot(i+1,1)];
    W_dot_tilda = Func_Tilda(Wdot);

    % Equation for acceleration analysis at head cg
    Rp_ddot =
Q_ddot(1:3)+(Func_Y_A(Q)*W_dot_tilda+Func_Y_A(Q)*W_tilda*W_tilda)* s;
    rpx_ddotG(i+1,1)=Rp_ddot(1,1);
    rpy_ddotG(i+1,1)=Rp_ddot(2,1);
    rpz_ddotG(i+1,1)=Rp_ddot(3,1);

    % Acceleration analysis New
    s_tilda = Func_Tilda(s);
    NRp_ddot = Q_ddot(1:3)-
Func_Y_A(Q)*s_tilda*[Wx_dot(i+1,1);Wy_dot(i+1,1);Wz_dot(i+1,1)]-
Func_Y_A(Q)*W_tilda*s_tilda*[Wx(i+1,1);Wy(i+1,1);Wz(i+1,1)];
    Nrpx_ddotG(i+1,1)=NRp_ddot(1,1);
    Nrpy_ddotG(i+1,1)=NRp_ddot(2,1);
    Nrpz_ddotG(i+1,1)=NRp_ddot(3,1);

    % Transform Angular acceleration to global coordinate system
    W_dotG = Func_Y_A(Q)*W_dot_tilda*Func_Y_A(Q)';
    Wx_dotG(i+1,1) = W_dotG(3,2);
    Wy_dotG(i+1,1) = W_dotG(1,3);
    Wz_dotG(i+1,1) = W_dotG(2,1);

    % Transform angular velocity (BFC) to 1st deritative of Euler angle
    % 1st derivative of Euler angle, Euler_dot (not global angular velocity)
    H = Func_Y_H(Q);
    Euler_dot = inv(H)*[Wx(i+1,1);Wy(i+1,1);Wz(i+1,1)];
    Phi31_dot(i+1,1)=Euler_dot(1,1);
    Phi11_dot(i+1,1)=Euler_dot(2,1);
    Phi32_dot(i+1,1)=Euler_dot(3,1);

    % Check the WxG,WyG,WzG using the other equation
    WG = Func_Y_A(Q)*W_tilda*Func_Y_A(Q)';
    WxG(i+1,1)= WG(3,2);
    WyG(i+1,1)= WG(1,3);
    WzG(i+1,1)= WG(2,1);

    % Global Angular Displacement
    AnDxG(i+1,1)=AnDxG(i,1)+0.5*(WxG(i,1)+WxG(i+1,1))*t_step;
    AnDyG(i+1,1)=AnDyG(i,1)+0.5*(WyG(i,1)+WyG(i+1,1))*t_step;
    AnDzG(i+1,1)=AnDzG(i,1)+0.5*(WzG(i,1)+WzG(i+1,1))*t_step;

    % Check the Wx, Wy, Wz (body fixed coordinate)
    A1 = Func_Y_A(Q);
    WGg = [WxG(i+1,1);WyG(i+1,1);WzG(i+1,1)];
    RWG_tilda = Func_Tilda(WGg);
    B1 = A1'*RWG_tilda*A1;
    TWx(i+1,1) = B1(3,2);
    TWy(i+1,1) = B1(1,3);
    TWz(i+1,1) = B1(2,1);

    % DISPLACEMENT (Updating generalized coordinate)
    % Update Euler angle by integrating 1st derivative of Euler angle
```

```
    V = V +
0.5*[Phi31_dot(i,1)+Phi31_dot(i+1,1);Phi11_dot(i,1)+Phi11_dot(i+1,1);Phi32_do
t(i,1)+Phi32_dot(i+1,1)]*t_step;
    phi_s1(i+1,1)= V(1,1);
    phi_s2(i+1,1)= V(2,1);
    phi_s3(i+1,1)= V(3,1);

    U = U +
0.5*[VxG(i,1)+VxG(i+1,1);VyG(i,1)+VyG(i+1,1);VzG(i,1)+VzG(i+1,1)]*t_step;
    DxG(i+1,1)=U(1,1);
    DyG(i+1,1)=U(2,1);
    DzG(i+1,1)=U(3,1);

    % Generalized coordinate system
    Q = [U;V];

    % Time update
    Time(i+1,1)=t;
    i=i+1;
end

% Time channel (ms)
Time_msec = Time*1000; % sec -> msec

% Euler angle (2(s1)-1(s2)-3(s3))
J211Euler2 =  (phi_s2)*180/pi; % rad -> deg
J211Euler1 =  (phi_s1)*180/pi; % rad -> deg
J211Euler3 =  (phi_s3)*180/pi; % rad -> deg

J211Rotx =  (AnDxG-AnDxG(1,1))*180/pi; % rad -> deg
J211Roty =  (AnDyG-AnDyG(1,1))*180/pi; % rad -> deg
J211Rotz =  (AnDzG-AnDzG(1,1))*180/pi; % rad -> deg

% Global(Lab coordinate) Position
J211Dx =  (rpxG-rpxG(1,1))*1000; % m -> mm
J211Dy =  (rpyG-rpyG(1,1))*1000; % m -> mm
J211Dz =  (rpzG-rpzG(1,1))*1000; % m -> mm

% Global(Lab coordinate) Angular Velocity
% rad/sec
J211AnVxR =  (WxG-WxG(1,1)); % rad/sec
J211AnVyR =  (WyG-WyG(1,1)); % rad/sec
J211AnVzR =  (WzG-WzG(1,1)); % rad/sec
% deg/sec
J211AnVxD =  (WxG-WxG(1,1))*180/pi; % rad/sec -> deg/sec
J211AnVyD =  (WyG-WyG(1,1))*180/pi; % rad/sec -> deg/sec
J211AnVzD =  (WzG-WzG(1,1))*180/pi; % rad/sec -> deg/sec

% Global(Lab coordinate) Linear Velocity
J211Vx =  (rpx_dotG-rpx_dotG(1,1)); % m/sec
J211Vy =  (rpy_dotG-rpy_dotG(1,1)); % m/sec
J211Vz =  (rpz_dotG-rpz_dotG(1,1)); % m/sec

% Global(Lab coordinate) Angular Acceleration
% rad/sec^2
```

```
J211AnAxR =  (Wx_dotG-Wx_dotG(1,1)); % rad/sec^2
J211AnAyR =  (Wy_dotG-Wy_dotG(1,1)); % rad/sec^2
J211AnAzR =  (Wz_dotG-Wz_dotG(1,1)); % rad/sec^2

% deg/sec^2
J211AnAxD =  (Wx_dotG-Wx_dotG(1,1))*180/pi; % rad/sec^2 -> deg/sec^2
J211AnAyD =  (Wy_dotG-Wy_dotG(1,1))*180/pi; % rad/sec^2 -> deg/sec^2
J211AnAzD =  (Wz_dotG-Wz_dotG(1,1))*180/pi; % rad/sec^2 -> deg/sec^2

% Global(Lab coordinate) Linear Acceleration
% g
J211Axg =  (rpx_ddotG-rpx_ddotG(1,1))/9.81; % m/sec^2 -> g
J211Ayg =  (rpy_ddotG-rpy_ddotG(1,1))/9.81; % m/sec^2 -> g
J211Azg =  (rpz_ddotG-rpz_ddotG(1,1))/9.81; % m/sec^2 -> g

% m/sec^2
J211AxM =  (rpx_ddotG-rpx_ddotG(1,1)); % m/sec^2
J211AyM =  (rpy_ddotG-rpy_ddotG(1,1)); % m/sec^2
J211AzM =  (rpz_ddotG-rpz_ddotG(1,1)); % m/sec^2

% Double check Global acceleration
% Compare this with J211 AxM, AyM, AzM: should be same
% g
J211NAxg =  (Nrpx_ddotG-Nrpx_ddotG(1,1))/9.81;
J211NAyg =  (Nrpy_ddotG-Nrpy_ddotG(1,1))/9.81;
J211NAzg =  (Nrpz_ddotG-Nrpz_ddotG(1,1))/9.81;

% Save Data
ThrAW_Poc_Dx =
[Time,Time_msec,J211Dx,J211Dy,J211Dz,J211Rotx,J211Roty,J211Rotz,J211Euler1,J2
11Euler2,J211Euler3];
ThrAW_Poc_Vx =
[J211Vx,J211Vy,J211Vz,J211AnVxR,J211AnVyR,J211AnVzR,J211AnVxD,J211AnVyD,J211A
nVzD];
ThrAW_Poc_Ax =
[J211Axg,J211Ayg,J211Azg,J211AxM,J211AyM,J211AzM,J211AnAxR,J211AnAyR,J211AnAz
R,J211AnAxD,J211AnAyD,J211AnAzD];
ThrAW_Poc = [ThrAW_Poc_Dx,ThrAW_Poc_Vx,ThrAW_Poc_Ax];

% Output name and unit--> copy and paste
%
Time,Time(msec),Dx,Dy,Dz,Rotx,Roty,Rotz,Euler1,Euler2,Euler3,Vx,Vy,Vz,AnVxR,A
nVyR,AnVzR,AnVxD,AnVyD,AnVzD,Axg,Ayg,Azg,AxM,AyM,AzM,AnAxR,AnAyR,AnAzR,AnAxD,
AnAyD,AnAzD
%
sec,msec,mm,mm,mm,deg,deg,deg,deg,deg,deg,m/sec,m/sec,m/sec,rad/sec,rad/sec,r
ad/sec,deg/sec,deg/sec,deg/sec,g,g,g,m/sec^2,m/sec^2,m/sec^2,rad/sec^2,rad/se
c^2,rad/sec^2,deg/sec^2,deg/sec^2,deg/sec^2
save PMHS3aw_proc.dat ThrAW_Poc -ascii
```